Stochastic analysis of flow in a heterogeneous unsaturated-saturated system

Dongxiao Zhang and Zhiming Lu

Hydrology, Geochemistry, and Geology Group, Los Alamos National Laboratory, Los Alamos, New Mexico, USA

Received 14 March 2001; revised 27 August 2001; accepted 30 August 2001; published 28 February 2002.

[1] In this study we develop a stochastic model for transient unsaturated-saturated flow in randomly heterogeneous media with the method of moment equations. We first derive partial differential equations governing the statistical moments of the flow quantities by perturbation expansions and then implement these equations under general conditions with the method of finite differences. The stochastic model developed is applicable to the entire domain of a bounded, multidimensional unsaturated-saturated system in the presence of random or deterministic recharge and sink/source and in the presence of multiscale, nonstationary medium features. The unsaturated and saturated zones are coupled through the water table, whose position is random in randomly heterogeneous porous media. The presence of the water table renders the flow moments strongly nonstationary even in the absence of medium nonstationary features. This finding is confirmed with Monte Carlo simulations. The resulting first two moments of flow may be used to approximate confidence intervals for the flow quantities. In addition, the integrated stochastic flow model provides the prerequisite quantities for realistically studying contaminant transport in unsaturated-saturated systems with a stochastic approach. *INDEX TERMS:* 1829 Hydrology: Groundwater hydrology; 1869 Hydrology: Stochastic processes; 1875 Hydrology: Unsaturated zone; 3220 Mathematical Geophysics: Nonlinear dynamics; *KEYWORDS:* stochastic, saturated, unsaturated, flow, heterogeneity, multiscale

1. Introduction

[2] It is well known that medium heterogeneity significantly impacts fluid flow and solute transport in the subsurface. Many stochastic theories have been developed to study this phenomenon in saturated zones [e.g., *Gelhar and Axness*, 1983; *Dagan*, 1984, 1989; *Winter et al.*, 1984; *Neuman et al.*, 1987; *Graham and McLaughlin*, 1989; *Rubin*, 1990; *Gelhar*, 1993; *Shvidler*, 1993; *Cushman and Ginn*, 1993; *Osnes*, 1995; *Zhang and Neuman*, 1995; *Guadagnini and Neuman*, 1999a, 1999b; *Zhang*, 1998; *Zhang and Winter*, 1999] and in unsaturated zones [e.g., *Dagan and Bresler*, 1979; *Bresler and Dagan*, 1981; *Andersson and Shapiro*, 1983; *Yeh et al.*, 1985a, 1985b; *Hopmans et al.*, 1988; *Destouni and Cvetkovic*, 1989; *Polmann et al.*, 1991; *Mantoglou*, 1992; *Indelman et al.*, 1993; *Kiefer*, 1993; *Liedl*, 1994; *Russo*, 1993, 1995a, 1995b; *Harter and Yeh*, 1996a, 1996b; *Zhang and Winter*, 1998; *Zhang et al.*, 1998; *Zhang*, 1999; *Tartakovsky et al.*, 1999; *Foussereau et al.*, 2000; *Lu et al.*, 2000]. A more detailed review of unsaturated flow models is given by *Zhang* [1999].

[3] It is common that stochastic theories are developed for either saturated or unsaturated systems. However, fluid flow and solute transport often occur in an integrated unsaturated and saturated system. Only a couple of stochastic studies considered flow and transport in such a situation. *Li and Yeh* [1998] investigated the sensitivity, the head variance, and the cross-correlation functions of the log hydraulic conductivity and pressure head for transient flow in a saturated-unsaturated system with a vector state-space approach. *Ferrante and Yeh* [1999] used the same approach to investigate the effect of uncertainty in boundary conditions and the effect of heterogeneity on pressure head and flux variance profiles for vertical transient unsaturated flows in one-dimensional domains. *Destouni and Graham* [1995] studied solute transport in an unsaturated-saturated flow system with a Lagrangian flux approach. However, in the latter study the requisite flow moments were directly taken as those that were developed separately for saturated and unsaturated domains without considering the coupling between them.

[4] In this study we develop a stochastic model for transient unsaturated-saturated flow with the method of moment equations in multiple dimensions. This is an extension of our nonstationary stochastic model for transient unsaturated flow [*Zhang*, 1999]. We first derive partial differential equations governing the statistical moments of the flow quantities by perturbation expansions and then implement these equations under general conditions with the method of finite differences. This approach is different from the state-space approach of *Li and Yeh* [1998] and *Ferrante and Yeh* [1999]: The former first derives the moment equations and then solves them numerically; the latter expresses the statistical moments on the basis of the spatial and temporal discretizations of a particular numerical scheme. Therefore, unlike the state-space approach, the moment equations derived in our approach are independent of the specific numerical scheme to be used and can be solved on numerical grids to be determined a posteriori based on the characteristics of the moment functions as well as on the particular configuration of a flow problem under consideration. The present study differs from *Li and Yeh* [1998] and *Zhang* [1999] in two more aspects. First, this study incorporates randomness in the initial/boundary conditions and source/sink terms. Second, it allows the input random fields to be nonstationary in space and time. Our study differs from *Ferrante and Yeh* [1999] in that we consider integrated unsaturated-saturated flows in multiple dimensions instead of one-dimensional unsaturated flows. The stochastic model developed in this study is applicable to the entire domain of a bounded, multidimensional unsaturated-saturated system in

the presence of random or deterministic recharge and sink/source as well as in the presence of multiscale, nonstationary medium features.

2. Stochastic Differential Equations

[5] We consider transient flow in unsaturated-saturated media satisfying the following continuity equation and Darcy's law:

$$\{S_s H(\psi) + H(-\psi) C[\psi,\cdot]\}\frac{\partial \psi(\mathbf{x},t)}{\partial t} + \nabla\cdot\mathbf{q}(\mathbf{x},t) = g(\mathbf{x},t) \quad (1)$$

$$q_i(\mathbf{x},t) = -K[\psi,\cdot]\frac{\partial}{\partial x_i}[\psi(\mathbf{x},t) + x_1], \quad (2)$$

subject to initial and boundary conditions

$$\psi(\mathbf{x},0) = \Psi_0(\mathbf{x}) \qquad \mathbf{x}\in\Omega \quad (3)$$

$$\psi(\mathbf{x},t) = \Psi(\mathbf{x},t), \qquad \mathbf{x}\in\Gamma_D \quad (4)$$

$$\mathbf{q}(\mathbf{x},t)\cdot\mathbf{n}(\mathbf{x}) = Q(\mathbf{x},t), \qquad \mathbf{x}\in\Gamma_N, \quad (5)$$

where $\mathbf{q}$ is the specific discharge (flux); $\psi(\mathbf{x}, t) + x_1$ is the total head; ψ is the pressure head; $i = 1,\ldots, d$ (where d is the number of space dimensions); $\Psi_0(\mathbf{x})$ is the initial pressure head in the domain Ω; $\Psi(\mathbf{x}, t)$ is the prescribed head on Dirichlet boundary segments Γ_D; $Q(\mathbf{x}, t)$ is the prescribed flux across Neuman boundary segments Γ_N; $\mathbf{n}(\mathbf{x}) = (n_1,\ldots,n_d)^T$ is an outward unit vector normal to the boundary; H(ψ) is the Heaviside step function, being zero when $\psi < 0$ and one when $\psi \geq 0$; S_S is the specific storage; $C[\psi,\cdot] = d\theta_e/d\psi$ is the specific moisture capacity; and $K[\psi,\cdot]$ is the unsaturated hydraulic conductivity (assumed to be isotropic locally). Both C and K are functions of pressure head and soil properties at $\mathbf{x}$. For convenience, they will be written as $C(\mathbf{x}, t)$ and $K(\mathbf{x}, t)$ in the sequel. The elevation x_1 is directed vertically upward. In these coordinates, recharge has negative sign. The seepage velocity at $\mathbf{x}$ is related to the specific flux q_i by

$$u_i(\mathbf{x},t) = \frac{q_i(\mathbf{x},t)}{\theta_e(\mathbf{x},t)}, \quad (6)$$

where $\theta_e \equiv \theta_e[\psi(\mathbf{x}, t),\cdot]$ is the effective volumetric water content at $\mathbf{x}$, which depends on ψ and soil properties when $\psi < 0$ and becomes the saturated water content θ_s when $\psi \geq 0$. It is clear that (1)–(5) become the governing equations for transient unsaturated flow if $\psi < 0$ and those for transient saturated flow if $\psi \geq 0$.

[6] It is clear that some model is needed to describe the constitutive relationships of K versus ψ and θ_e versus ψ when the flow is unsaturated. No universal models are available for the constitutive relationships. Instead, several empirical models are usually used, including the Gardner-Russo model [*Gardner*, 1958; *Russo*, 1988], the Brooks-Corey model [*Brooks and Corey*, 1964], and the van Genuchten–Mualem model [*van Genuchten*, 1980]. In most previous stochastic models of unsaturated flow, the Gardner-Russo model is used because of simplicity. Although the Brooks-Corey model may have certain mathematical advantages over the Gardner-Russo model in low-order stochastic analyses [*Zhang et al.*, 1998], we use the latter to facilitate comparisons with literature results. The Gardner-Russo model reads as

$$K(\mathbf{x},t) = K_s(\mathbf{x})\exp[\alpha(\mathbf{x})\psi(\mathbf{x},t)] \quad (7)$$

$$\theta_e(\mathbf{x},t) = (\theta_s - \theta_r)\{\exp[0.5\alpha(\mathbf{x})\psi(\mathbf{x},t)][1 - 0.5\alpha(\mathbf{x})\psi(\mathbf{x},t)]\}^{2/(m+2)}, \quad (8)$$

where $\psi \leq 0$. In the above, α is the soil parameter related to pore size distribution, m is a parameter related to tortuosity (taken to be known), θ_r is the residual (irreducible) water content, and θ_s is the saturated water content. The variabilities of θ_s and θ_r are likely to be small compared with that of the effective water content θ_e [*Russo and Bouton*, 1992]. With (8), $C(\mathbf{x}, t) = d\theta_e/d\psi$ can be expressed explicitly.

[7] In this study, θ_s, θ_r, and m are assumed to be deterministic constants, while the soil parameter $\alpha(\mathbf{x})$ and log transformed saturated hydraulic conductivity $f(\mathbf{x}) = \ln K_s(\mathbf{x})$ are treated as random space functions. We also allow spatial variability and/or randomness in the initial and boundary terms $\Psi_0(\mathbf{x})$, $\Psi(\mathbf{x}, t)$, and $Q(\mathbf{x}, t)$ and in the source/sink term $g(\mathbf{x}, t)$. They are generally treated as (spatially and/or temporally) nonstationary random space functions (random fields). Thus the expected values may be space-time dependent, and the covariances may depend on the actual points in space-time rather than only on their space-time lags. For example, multiscale medium features such as distinct soil layers, zones, and facies may cause the soil properties $f(\mathbf{x})$ and $\alpha(\mathbf{x})$ to be spatially nonstationary, seasonal variations may render the net recharge rate $Q(\mathbf{x}, t)$ temporally nonstationary, and additional variations in vegetation coverage may lead to spatial and temporal nonstationarities in Q (due to evapotranspiration among other factors). Also, a stationary random field becomes nonstationary after conditioning on measurements. A detailed discussion on nonstationary random fields is given by *Zhang* [2002].

[8] When the soil properties $f(\mathbf{x})$ and $\alpha(\mathbf{x})$, the initial/boundary conditions $\Psi_0(\mathbf{x})$, $\Psi(\mathbf{x}, t)$, and $Q(\mathbf{x}, t)$, and/or the source/sink terms $g(\mathbf{x}, t)$ are treated as random functions, the governing equations (1)–(5) become a set of stochastic partial differential equations whose solutions are no longer deterministic values but probability distributions or related quantities such as statistical moments of the dependent variables. In the next section we derive equations governing the first two moments (means and covariances) of the flow quantities in an unsaturated-saturated system. For simplicity, we assume the various random variables $g(\mathbf{x}, t)$, $\Psi_0(\mathbf{x})$, $\Psi(\mathbf{x}, t)$, and $Q(\mathbf{x}, t)$ to be mutually independent and to be uncorrelated with the soil properties $f(\mathbf{x})$ and $\alpha(\mathbf{x})$.

3. Moment Differential Equations

[9] As is commonly done, we work with the log transformed unsaturated hydraulic conductivity $Y(\mathbf{x}, t) = \ln K(\mathbf{x}, t)$, which is equal to $f(\mathbf{x}) + \alpha(\mathbf{x})\psi(\mathbf{x}, t)$ (where $f = \ln K_s(\mathbf{x})$) for $\psi < 0$ and $f(\mathbf{x})$ for $\psi \geq 0$. It may be written in a general form as

$$Y(\mathbf{x},t) = f(\mathbf{x}) - R[-\psi(\mathbf{x},t)]\alpha(\mathbf{x}), \quad (9)$$

where $R(z) = zH(z)$ is the ramp function.

[10] Substituting (2) into (1) and utilizing $Y(\mathbf{x}, t) = \ln K(\mathbf{x}, t)$ yields

$$\frac{\partial^2\psi(\mathbf{x},t)}{\partial x_i^2} + \frac{\partial Y(\mathbf{x},t)}{\partial x_i}\left[\frac{\partial\psi(\mathbf{x},t)}{\partial x_i} + \delta_{i1}\right] = C_s(\mathbf{x},t)e^{-Y(\mathbf{x},t)}\frac{\partial\psi(\mathbf{x},t)}{\partial t} - g(\mathbf{x},t)e^{-Y(\mathbf{x},t)} \quad (10)$$

$$\psi(\mathbf{x},0)=\Psi_0(\mathbf{x}),\qquad \mathbf{x}\in\Omega \tag{11}$$

$$\psi(\mathbf{x},t)=\Psi(\mathbf{x},t),\qquad \mathbf{x}\in\Gamma_D \tag{12}$$

$$n_i(\mathbf{x})e^{Y(\mathbf{x},t)}\left[\frac{\partial\psi(\mathbf{x},t)}{\partial x_i}+\delta_{i1}\right]=-Q(\mathbf{x},t),\qquad \mathbf{x}\in\Gamma_N, \tag{13}$$

where $C_s(\mathbf{x},t)=S_sH[\psi(\mathbf{x},t)]+H[-\psi(\mathbf{x},t)]C(\mathbf{x},t)$ and δ_{i1} is the Kronecker delta function. Summation for repeated indices is implied. Because the variability of $\psi(\mathbf{x},t)$ depends on the input variabilities, i.e., those of the soil properties f and α and those of the initial/boundary and source/sink terms, and the variabilities of Y and C_s depend on those of ψ and the input variables, one may express these quantities as infinite series in the following form: $\psi(\mathbf{x},t)=\psi^{(0)}+\psi^{(1)}+\psi^{(2)}+\ldots$, $Y(\mathbf{x},t)=Y^{(0)}+Y^{(1)}+Y^{(2)}+\ldots$, and $C_s(\mathbf{x},t)=C_s^{(0)}+C_s^{(1)}+C_s^{(2)}+\ldots$. In these series, the order of each term is with respect to σ, which, to be clear later, is some combination of the variabilities of the input variables. After substituting these and the following formal decompositions into (10)–(13): $g(\mathbf{x},t)=\langle g(\mathbf{x},t)\rangle+g'(\mathbf{x},t)$, $\Psi_0(\mathbf{x})=\langle\Psi_0(\mathbf{x})\rangle+\Psi_0'(\mathbf{x})$, $\Psi(\mathbf{x},t)=\langle\Psi(\mathbf{x},t)\rangle+\Psi'(\mathbf{x},t)$, and $Q(\mathbf{x},t)=\langle Q(\mathbf{x},t)\rangle+Q'(\mathbf{x},t)$, and collecting terms at separate order, we obtain

$$\frac{\partial^2\psi^{(0)}(\mathbf{x},t)}{\partial x_i^2}+\frac{\partial Y^{(0)}(\mathbf{x},t)}{\partial x_i}\left[\frac{\partial\psi^{(0)}(\mathbf{x},t)}{\partial x_i}+\delta_{i1}\right]=\frac{C_s^{(0)}(\mathbf{x},t)}{K_m(\mathbf{x},t)}\frac{\partial\psi^{(0)}(\mathbf{x},t)}{\partial t}-\frac{\langle g(\mathbf{x},t)\rangle}{K_m(\mathbf{x},t)} \tag{14}$$

$$\psi^{(0)}(\mathbf{x},0)=\langle\psi_0(\mathbf{x})\rangle,\qquad \mathbf{x}\in\Omega \tag{15}$$

$$\psi^{(0)}(\mathbf{x},t)=\langle\psi(\mathbf{x},t)\rangle,\qquad \mathbf{x}\in\Gamma_D \tag{16}$$

$$n_i(\mathbf{x})\left[\frac{\partial\psi^{(0)}(\mathbf{x},t)}{\partial x_i}+\delta_{i1}\right]=-\frac{\langle Q(\mathbf{x},t)\rangle}{K_m(\mathbf{x},t)},\qquad \mathbf{x}\in\Gamma_N \tag{17}$$

$$\begin{aligned}&\frac{\partial^2\psi^{(1)}(\mathbf{x},t)}{\partial x_i^2}+J_i(\mathbf{x},t)\frac{\partial Y^{(1)}(\mathbf{x},t)}{\partial x_i}+\frac{\partial Y^{(0)}(\mathbf{x},t)}{\partial x_i}\frac{\partial\psi^{(1)}(\mathbf{x},t)}{\partial x_i}\\&=\frac{C_s^{(0)}(\mathbf{x},t)}{K_m(\mathbf{x},t)}\left[\frac{\partial\psi^{(1)}(\mathbf{x},t)}{\partial t}-J_t(\mathbf{x},t)Y^{(1)}(\mathbf{x},t)\right]+\frac{C_s^{(1)}(\mathbf{x},t)}{K_m(\mathbf{x},t)}J_t(\mathbf{x},t)\\&+\frac{1}{K_m(\mathbf{x},t)}\left[\langle g(\mathbf{x},t)\rangle Y^{(1)}(\mathbf{x},t)-g'(\mathbf{x},t)\right]\end{aligned} \tag{18}$$

$$\psi^{(1)}(\mathbf{x},0)=\Psi_0'(\mathbf{x}),\qquad \mathbf{x}\in\Omega \tag{19}$$

$$\psi^{(1)}(\mathbf{x},t)=\Psi'(\mathbf{x},t),\qquad \mathbf{x}\in\Gamma_D \tag{20}$$

$$n_i(\mathbf{x})\left[\frac{\partial\psi^{(1)}(\mathbf{x},t)}{\partial x_i}+J_i(\mathbf{x},t)Y^{(1)}(\mathbf{x},t)\right]=-\frac{Q'(\mathbf{x},t)}{K_m(\mathbf{x},t)}\qquad \mathbf{x}\in\Gamma_N \tag{21}$$

$$\begin{aligned}&\frac{\partial^2\psi^{(2)}(\mathbf{x},t)}{\partial x_i^2}+\frac{\partial Y^{(0)}(\mathbf{x},t)}{\partial x_i}\frac{\partial\psi^{(2)}(\mathbf{x},t)}{\partial x_i}\\&=\frac{C_s^{(0)}}{K_m(\mathbf{x},t)}\frac{\partial\psi^{(2)}(\mathbf{x},t)}{\partial t}-\frac{\partial Y^{(1)}(\mathbf{x},t)}{\partial x_i}\frac{\partial\psi^{(1)}(\mathbf{x},t)}{\partial x_i}\\&-J_i(\mathbf{x},t)\frac{\partial Y^{(2)}(\mathbf{x},t)}{\partial x_i}+\frac{C_s^{(2)}}{K_m(\mathbf{x},t)}J_t(\mathbf{x},t)\\&+\frac{C_s^{(1)}}{K_m(\mathbf{x},t)}\left[\frac{\partial\psi^{(1)}(\mathbf{x},t)}{\partial t}-Y^{(1)}(\mathbf{x},t)J_t(\mathbf{x},t)\right]\\&-\frac{C_s^{(0)}}{K_m(\mathbf{x},t)}\left\{Y^{(1)}(\mathbf{x},t)\frac{\partial\psi^{(1)}(\mathbf{x},t)}{\partial t}-J_t(\mathbf{x},t)\right.\\&\left.\left[Y^{(2)}(\mathbf{x},t)-\frac{1}{2}\left(Y^{(1)}(\mathbf{x},t)\right)^2\right]\right\}+\frac{1}{K_m(\mathbf{x},t)}\\&\left\{g'(\mathbf{x},t)Y^{(1)}(\mathbf{x},t)+\langle g(\mathbf{x},t)\rangle\right.\\&\left.\left[Y^{(2)}(\mathbf{x},t)-\frac{1}{2}\left(Y^{(1)}(\mathbf{x},t)\right)^2\right]\right\}\end{aligned} \tag{22}$$

$$\psi^{(2)}(\mathbf{x},0)=0,\quad \mathbf{x}\in\Omega \tag{23}$$

$$\psi^{(2)}(\mathbf{x},t)=0,\quad \mathbf{x}\in\Gamma_D \tag{24}$$

$$n_i(\mathbf{x})\left\{\frac{\partial\psi^{(2)}(\mathbf{x},t)}{\partial x_i}+Y^{(1)}(\mathbf{x},t)\frac{\partial\psi^{(1)}(\mathbf{x},t)}{\partial x_i}+J_i(\mathbf{x},t)\left[Y^{(2)}(\mathbf{x},t)+\frac{1}{2}\left(Y^{(1)}(\mathbf{x},t)\right)^2\right]\right\}=0,\ \mathbf{x}\in\Gamma_N, \tag{25}$$

where $K_m(\mathbf{x},t)=\exp[Y^{(0)}(\mathbf{x},t)]$ and $J_i(\mathbf{x},t)=\partial\psi^{(0)}(\mathbf{x},t)/\partial x_i+\delta_{i1}$ and $J_t(\mathbf{x},t)=\partial\psi^{(0)}(\mathbf{x},t)/\partial t$ are the respective spatial and temporal mean gradient of (total) head. It can be shown that $\langle\psi^{(0)}\rangle=\psi^{(0)}$ and $\langle\psi^{(1)}\rangle=0$. Hence the mean pressure head is $\langle\psi\rangle=\psi^{(0)}$ to zeroth or first order in σ and $\langle\psi\rangle=\psi^{(0)}+\langle\psi^{(2)}\rangle$ to second order. The head fluctuation is $\psi'=\psi^{(1)}$ to first order. Therefore the head covariance is $C_\psi(\mathbf{x},t;\chi,\tau)=\langle\psi^{(1)}(\mathbf{x},t)\psi^{(1)}(\chi,\tau)\rangle$ to first order in σ^2 (or second order in σ).

[11] On the basis of (9), it is shown (Appendix A) that

$$Y^{(0)}(\mathbf{x},t)=\langle f(\mathbf{x})\rangle-\langle\alpha(\mathbf{x})\rangle R\left[-\psi^{(0)}(\mathbf{x},t)\right] \tag{26}$$

$$\begin{aligned}Y^{(1)}(\mathbf{x},t)=&f'(\mathbf{x})+H\left[-\psi^{(0)}(\mathbf{x},t)\right]\\&\cdot\left[\langle\alpha(\mathbf{x})\rangle\psi^{(1)}(\mathbf{x};t)+\psi^{(0)}(\mathbf{x},t)\alpha'(\mathbf{x})\right]\end{aligned} \tag{27}$$

$$\begin{aligned}Y^{(2)}(\mathbf{x},t)=&\langle\alpha(\mathbf{x})\rangle H\left[-\psi^{(0)}(\mathbf{x},t)\right]\psi^{(2)}(\mathbf{x},t)+H\left[-\psi^{(0)}(\mathbf{x},t)\right]\\&\cdot\alpha'(\mathbf{x})\psi^{(1)}(\mathbf{x},t)-\frac{1}{2}\langle\alpha(\mathbf{x})\rangle\\&\cdot\delta\left[-\psi^{(0)}(\mathbf{x},t)\right]\left[\psi^{(1)}(\mathbf{x},t)\right]^2.\end{aligned} \tag{28}$$

[12] As $C_s(\mathbf{x},t)$ is, in general, a function of the two random variables ψ and α, we may expand by Taylor expansion with respect to $\psi^{(0)}$ and $\langle\alpha(\mathbf{x})\rangle$. It can be verified that this procedure leads to

$$C_s^{(0)}=S_sH\left(\psi^{(0)}\right)+H\left(-\psi^{(0)}\right)p_{00} \tag{29}$$

$$C_s^{(1)}=C_1\psi^{(1)}(\mathbf{x},t)+H\left(-\psi^{(0)}\right)p_{01}\alpha'(\mathbf{x},t) \tag{30}$$

$$\begin{aligned}C_s^{(2)}=&C_1\psi^{(2)}(\mathbf{x},t)+\frac{1}{2}\left\{S_s\delta\left(\psi^{(0)}\right)+H\left(-\psi^{(0)}\right)p_{20}\right.\\&\left.+\delta'\left(-\psi^{(0)}\right)p_{00}-\delta\left(-\psi^{(0)}\right)p_{10}\right\}\left[\psi^{(1)}\right]^2\\&+\frac{1}{2}H\left(-\psi^{(0)}\right)p_{02}[\alpha'(\mathbf{x},t)]^2+\frac{1}{2}H\left(-\psi^{(0)}\right)\\&\cdot p_{11}\alpha'(\mathbf{x},t)\psi^{(1)}(\mathbf{x},t).\end{aligned} \tag{31}$$

Here $p_{ij} = \partial^{i+j}C(\mathbf{x}, t)/\partial\psi^i\partial\alpha^j$ evaluated at $\langle\alpha(\mathbf{x})\rangle$ and $\psi^{(0)}$, and $C_1 = S_s\delta(\psi^{(0)}) + H(-\psi^{(0)})p_{10} - \delta(-\psi^{(0)})p_{00}$.

[13] Substituting (26) and (29) into (14)–(17) yields

$$\frac{\partial^2\psi^{(0)}(\mathbf{x},t)}{\partial x_i^2} + a_i(\mathbf{x},t)\frac{\partial\psi^{(0)}(\mathbf{x},t)}{\partial x_i} + c_2(\mathbf{x},t)\psi^{(0)}(\mathbf{x},t) = -\frac{\langle g(\mathbf{x},t)\rangle}{K_m(\mathbf{x},t)} + e(\mathbf{x},t)\frac{\partial\psi^{(0)}(\mathbf{x},t)}{\partial t} + d_6(\mathbf{x},t) \tag{32}$$

$$\psi^{(0)}(\mathbf{x},0) = \langle\Psi_0(\mathbf{x})\rangle, \qquad \mathbf{x}\in\Omega \tag{33}$$

$$\psi^{(0)}(\mathbf{x},t) = \langle\Psi(\mathbf{x},t)\rangle, \qquad \mathbf{x}\in\Gamma_D \tag{34}$$

$$n_i(\mathbf{x})\left[\frac{\partial\psi^{(0)}(\mathbf{x},t)}{\partial x_i}\right] = -\frac{\langle Q(\mathbf{x},t)\rangle}{K_m(\mathbf{x},t)} - \delta_{i1}n_i(\mathbf{x}), \qquad \mathbf{x}\in\Gamma_N, \tag{35}$$

where

$$\begin{aligned} K_m(\mathbf{x},t) &= \exp[\langle f(\mathbf{x})\rangle]\exp\left\{H\left[-\psi^{(0)}(\mathbf{x},t)\right]\langle\alpha(\mathbf{x})\rangle\psi^{(0)}(x,t)\right\};\\ a_i(\mathbf{x},t) &= \langle\alpha(\mathbf{x})\rangle H\left[-\psi^{(0)}(\mathbf{x},t)\right]J_i(\mathbf{x},t);\\ c_2(\mathbf{x},t) &= J_i(\mathbf{x},t)H\left[-\psi^{(0)}(\mathbf{x},t)\right]\partial\langle\alpha(\mathbf{x})\rangle/\partial\mathbf{x}_i;\\ d_6(\mathbf{x},t) &= -J_i(\mathbf{x},t)\partial\langle f(\mathbf{x})\rangle/\partial\mathbf{x}_i;\\ e\ (\mathbf{x},t) &= C_s^{(0)}\Big/K_m(\mathbf{x},t). \end{aligned} \tag{36}$$

It is clear that (32) is nonlinear at the unsaturated regime (i.e., $\psi^{(0)} < 0$) and becomes linear at the saturated regime (i.e., $\psi^{(0)} \geq 0$). This transition is expressed mathematically with the Heaviside step function.

[14] Substituting (27) and (30) into (18)–(21) yields

$$\begin{aligned} &\frac{\partial^2\psi^{(1)}(\mathbf{x},t)}{\partial x_i^2} + b_i(\mathbf{x},t)\frac{\partial\psi^{(1)}(\mathbf{x},t)}{\partial x_i} + c(\mathbf{x},t)\psi^{(1)}(\mathbf{x},t)\\ &= e(\mathbf{x},t)\frac{\partial\psi^{(1)}(\mathbf{x},t)}{\partial t} - J_i(\mathbf{x},t)\frac{\partial f'(\mathbf{x})}{\partial x_i} - H\left(-\psi^{(0)}\right)\\ &\cdot J_i(\mathbf{x},t)\psi^{(0)}(\mathbf{x},t)\frac{\partial\alpha'(\mathbf{x})}{\partial x_i} + d_1(\mathbf{x},t)f'(\mathbf{x})\\ &+ d_2(\mathbf{x},t)\alpha'(\mathbf{x}) - \frac{1}{K_m(\mathbf{x},t)}g'(\mathbf{x},t) \end{aligned} \tag{37}$$

$$\psi^{(1)}(\mathbf{x},0) = \Psi_0'(\mathbf{x}), \qquad \mathbf{x}\in\Omega \tag{38}$$

$$\psi^{(1)}(\mathbf{x},t) = \Psi'(\mathbf{x},t), \qquad \mathbf{x}\in\Gamma_D \tag{39}$$

$$n_i(\mathbf{x})\frac{\partial\psi^{(1)}(\mathbf{x},t)}{\partial x_i} + d_3(\mathbf{x},t)\psi^{(1)}(\mathbf{x},t) = d_4(\mathbf{x},t)f'(\mathbf{x}) + d_5(\mathbf{x},t)\alpha'(\mathbf{x}) - \frac{Q'(\mathbf{x},t)}{K_m(\mathbf{x},t)}, \qquad \mathbf{x}\in\Gamma_N \tag{40}$$

where

$$\begin{aligned} b_i(\mathbf{x},t) &= [2J_i(\mathbf{x},t) - \delta_{i1}]H\left(-\psi^{(0)}\right)\langle\alpha(\mathbf{x})\rangle + \frac{\partial\langle f(\mathbf{x})\rangle}{\partial x_i} - \frac{\partial\langle\alpha(\mathbf{x})\rangle}{\partial x_i}R\left(-\psi^{(0)}\right)\\ c(\mathbf{x},t) &= -\langle\alpha(\mathbf{x})\rangle H\left(-\psi^{(0)}\right)d_1(\mathbf{x},t) - C_1J_t(\mathbf{x},t)/K_m(\mathbf{x},t) + J_i\\ &\cdot(\mathbf{x},t)\left(H\left(-\psi^{(0)}\right)\frac{\partial\langle\alpha(\mathbf{x})\rangle}{\partial x_i} - \delta\left(-\psi^{(0)}\right)\langle\alpha(\mathbf{x})\rangle[J_i(\mathbf{x},t) - \delta_{i1}]\right)\\ d_1(\mathbf{x},t) &= \left(\langle g(\mathbf{x},t)\rangle - C_s^{(0)}(\mathbf{x},t)J_t(\mathbf{x},t)\right)\Big/K_m(\mathbf{x},t)\\ d_2(\mathbf{x},t) &= H\left(-\psi^{(0)}\right)\Big[d_1(\mathbf{x},t)\psi^{(0)}(\mathbf{x},t) - J_i(\mathbf{x},t)[J_i(\mathbf{x},t) - \delta_{i1}]\\ &\quad + J_t(\mathbf{x},t)p_{01}/K_m(\mathbf{x},t)\Big]\\ d_3(\mathbf{x},t) &= n_i(\mathbf{x})J_i(\mathbf{x},t)H\left(-\psi^{(0)}\right)\langle\alpha(\mathbf{x})\rangle\\ d_4(\mathbf{x},t) &= -n_i(\mathbf{x})J_i(\mathbf{x},t)\\ d_5(\mathbf{x},t) &= -n_i(\mathbf{x})J_i(\mathbf{x},t)H\left(-\psi^{(0)}\right)\psi^{(0)}(\mathbf{x},t). \end{aligned} \tag{41}$$

[15] Multiplying (37)–(40) by $\psi^{(1)}(\chi, \tau)$ and taking the ensemble mean yields equations for the covariance function of pressure head:

$$\begin{aligned} &\frac{\partial^2C_\psi(\mathbf{x},t;\boldsymbol{\chi},\tau)}{\partial x_i^2} + b_i(\mathbf{x},t)\frac{\partial C_\psi(\mathbf{x},t;\boldsymbol{\chi},\tau)}{\partial x_i} + c(\mathbf{x},t)C_\psi(\mathbf{x},t;\boldsymbol{\chi},\tau)\\ &= e(\mathbf{x},t)\frac{\partial C_\psi(\mathbf{x},t;\boldsymbol{\chi},\tau)}{\partial t} - J_i(\mathbf{x},t)\frac{\partial C_{f\psi}(\mathbf{x};\boldsymbol{\chi},\tau)}{\partial x_i}\\ &-H\left(-\psi^{(0)}\right)J_i(\mathbf{x},t)\psi^{(0)}(\mathbf{x},t)\frac{\partial C_{\alpha\psi}(\mathbf{x};\boldsymbol{\chi},\tau)}{\partial x_i}\\ &+ d_1(\mathbf{x},t)C_{f\psi}(\mathbf{x};\boldsymbol{\chi},\tau) + d_2(\mathbf{x},t)C_{\alpha\psi}(\mathbf{x};\boldsymbol{\chi},\tau)\\ &-\frac{1}{K_m(\mathbf{x},t)}C_{g\psi}(\mathbf{x},t;\boldsymbol{\chi},\tau) \end{aligned} \tag{42}$$

$$C_\psi(\mathbf{x},0;\boldsymbol{\chi},\tau) = C_{\Psi_0\psi}(\mathbf{x};\boldsymbol{\chi},\tau), \qquad \mathbf{x}\in\Omega \tag{43}$$

$$C_\psi(\mathbf{x},t;\boldsymbol{\chi},\tau) = C_{\Psi\psi}(\mathbf{x},t;\boldsymbol{\chi},\tau), \qquad \mathbf{x}\in\Gamma_D \tag{44}$$

$$n_i(\mathbf{x})\frac{\partial C_\psi(\mathbf{x},t;\boldsymbol{\chi},\tau)}{\partial x_i} + d_3(\mathbf{x},t)C_\psi(\mathbf{x},t;\boldsymbol{\chi},\tau) = d_4(\mathbf{x},t)C_{f\psi}(\mathbf{x};\boldsymbol{\chi},\tau) + d_5(\mathbf{x},t)C_{\alpha\psi}(\mathbf{x};\boldsymbol{\chi},\tau) - \frac{1}{K_m(\mathbf{x},t)}C_{Q\psi}(\mathbf{x},t;\boldsymbol{\chi},\tau), \qquad \mathbf{x}\in\Gamma_N, \tag{45}$$

where $C_{f\psi}$, $C_{\alpha\psi}$, $C_{g\psi}$, $C_{\Psi_0\psi}$, $C_{\Psi\psi}$, and $C_{Q\psi}$ can be formulated by multiplying $f'(\mathbf{x})$, $\alpha'(\mathbf{x})$, $g'(\mathbf{x},t)$, $\Psi'_0(\mathbf{x})$, $\Psi'(\mathbf{x},t)$, and $Q'(\mathbf{x},t)$ to (37)–(40), respectively, taking the ensemble mean, and recalling the assumption that f and α are independent of g, Ψ_0, Ψ, and Q,

$$\begin{aligned} &\frac{\partial^2C_{f\psi}(\mathbf{x};\boldsymbol{\chi},\tau)}{\partial\chi_i^2} + b_i(\boldsymbol{\chi},\tau)\frac{\partial C_{f\psi}(\mathbf{x};\boldsymbol{\chi},\tau)}{\partial\chi_i} + c(\boldsymbol{\chi},\tau)C_{f\psi}(\mathbf{x};\boldsymbol{\chi},\tau)\\ &= e(\boldsymbol{\chi},\tau)\frac{\partial C_{f\psi}(\mathbf{x};\boldsymbol{\chi},\tau)}{\partial\tau} - J_i(\boldsymbol{\chi},\tau)\frac{\partial C_f(x;\boldsymbol{\chi})}{\partial\boldsymbol{\chi}_i}\\ &+R\left(-\psi^{(0)}(\boldsymbol{\chi},\tau)\right)J_i(\boldsymbol{\chi},\tau)\frac{\partial C_{f\alpha}(\mathbf{x};\boldsymbol{\chi})}{\partial\boldsymbol{\chi}_i}\\ &+ d_1(\boldsymbol{\chi},\tau)C_f(\mathbf{x};\boldsymbol{\chi}) + d_2(\boldsymbol{\chi},\tau)C_{f\alpha}(\mathbf{x};\boldsymbol{\chi}) \end{aligned} \tag{46}$$

$$C_{f\Psi}\ (\mathbf{x};\boldsymbol{\chi},0) = C_{f\Psi_0}(\mathbf{x};\boldsymbol{\chi}), \qquad \boldsymbol{\chi}\in\Omega \tag{47}$$

$$C_{f\psi}\ (\mathbf{x};\boldsymbol{\chi},\tau) = C_{f\psi}(\mathbf{x};\boldsymbol{\chi},\tau), \qquad \boldsymbol{\chi}\in\Gamma_D \tag{48}$$

$$n_i(\boldsymbol{\chi})\frac{\partial C_{f\psi}(\mathbf{x};\boldsymbol{\chi},\tau)}{\partial\boldsymbol{\chi}_i} + d_3(\boldsymbol{\chi},\tau)C_{f\psi}(\mathbf{x};\boldsymbol{\chi},\tau) = d_4(\boldsymbol{\chi},\tau)C_f(\mathbf{x};\boldsymbol{\chi}) + d_5(\boldsymbol{\chi},\tau)C_{f\alpha}(\mathbf{x};\boldsymbol{\chi}), \qquad \boldsymbol{\chi}\in\Gamma_N \tag{49}$$

$$\frac{\partial^2 C_{\alpha\psi}(\mathbf{x};\boldsymbol{\chi},\tau)}{\partial \chi_i^2} + b_i(\boldsymbol{\chi},\tau)\frac{\partial C_{\alpha\psi}(\mathbf{x};\boldsymbol{\chi},\tau)}{\partial \chi_i} + c(\boldsymbol{\chi},\tau)C_{\alpha\psi}(\mathbf{x};\boldsymbol{\chi},\tau)$$
$$= e(\boldsymbol{\chi},\tau)\frac{\partial C_{\alpha\psi}(\mathbf{x};\boldsymbol{\chi},\tau)}{\partial \tau} - J_i(\boldsymbol{\chi},\tau)\frac{\partial C_{\alpha f}(\mathbf{x};\boldsymbol{\chi})}{\partial \boldsymbol{\chi}_i}$$
$$+ R\left(-\psi^{(0)}(\boldsymbol{\chi},\tau)\right)J_i(\boldsymbol{\chi},\tau)\frac{\partial C_{\alpha}(\mathbf{x};\boldsymbol{\chi})}{\partial \boldsymbol{\chi}_i}$$
$$+ d_1(\boldsymbol{\chi},\tau)C_{\alpha f}(\mathbf{x};\boldsymbol{\chi}) + d_2(\boldsymbol{\chi},\tau)C_{\alpha}(\mathbf{x};\boldsymbol{\chi}) \tag{50}$$

$$C_{\alpha\psi}(\mathbf{x};\boldsymbol{\chi},0) = C_{\alpha\Psi_0}(\mathbf{x};\boldsymbol{\chi}), \qquad \boldsymbol{\chi}\in\Omega \tag{51}$$

$$C_{\alpha\psi}(\mathbf{x};\boldsymbol{\chi},\tau) = C_{\alpha\Psi}(\mathbf{x};\boldsymbol{\chi},\tau), \qquad \boldsymbol{\chi}\in\Gamma_D \tag{52}$$

$$n_i(\boldsymbol{\chi})\frac{\partial C_{\alpha\psi}(\mathbf{x};\boldsymbol{\chi},\tau)}{\partial \chi_i} + d_3(\boldsymbol{\chi},\tau)C_{\alpha\psi}(\mathbf{x};\boldsymbol{\chi},\tau) = d_4(\boldsymbol{\chi},\tau)C_{\alpha f}(\mathbf{x};\boldsymbol{\chi})$$
$$+ d_5(\boldsymbol{\chi},\tau)C_{\alpha}(\mathbf{x};\boldsymbol{\chi}), \qquad \boldsymbol{\chi}\in\Gamma_N \tag{53}$$

$$\frac{\partial^2 C_{g\psi}(\mathbf{x},t;\boldsymbol{\chi},\tau)}{\partial \chi_i^2} + b_i(\boldsymbol{\chi},\tau)\frac{\partial C_{g\psi}(\mathbf{x},t;\boldsymbol{\chi},\tau)}{\partial \chi_i} + c(\boldsymbol{\chi},\tau)C_{g\psi}$$
$$\cdot(\mathbf{x},t;\boldsymbol{\chi},\tau) = e(\boldsymbol{\chi},\tau)\frac{\partial C_{g\psi}(\mathbf{x},t;\boldsymbol{\chi},\tau)}{\partial \tau}$$
$$-\frac{1}{K_m(\boldsymbol{\chi},\tau)}C_g(\mathbf{x},t;\boldsymbol{\chi},\tau) \tag{54}$$

$$C_{g\psi}(\mathbf{x},t;\boldsymbol{\chi},0) = 0, \qquad \boldsymbol{\chi}\in\Omega \tag{55}$$

$$C_{g\psi}(\mathbf{x},t;\boldsymbol{\chi},\tau) = 0, \qquad \boldsymbol{\chi}\in\Gamma_D \tag{56}$$

$$n_i(\boldsymbol{\chi})\frac{\partial C_{g\psi}(\mathbf{x},t;\boldsymbol{\chi},\tau)}{\partial \chi_i} + d_3(\boldsymbol{\chi},\tau)C_{g\psi}(\mathbf{x},t;\boldsymbol{\chi},\tau) = 0, \qquad \boldsymbol{\chi}\in\Gamma_N \tag{57}$$

$$\frac{\partial^2 C_{\Psi_0\psi}(\mathbf{x};\boldsymbol{\chi},\tau)}{\partial \chi_i^2} + b_i(\boldsymbol{\chi},\tau)\frac{\partial C_{\Psi_0\psi}(\mathbf{x};\boldsymbol{\chi},\tau)}{\partial \chi_i} + c(\boldsymbol{\chi},\tau)C_{\Psi_0\psi}(\mathbf{x};\boldsymbol{\chi},\tau)$$
$$= e(\boldsymbol{\chi},\tau)\frac{\partial C_{\Psi_0\psi}(\mathbf{x};\boldsymbol{\chi},\tau)}{\partial \tau} \tag{58}$$

$$C_{\Psi_0\psi}(\mathbf{x};\boldsymbol{\chi},0) = C_{\Psi_0}(\mathbf{x};\boldsymbol{\chi}), \qquad \boldsymbol{\chi}\in\Omega \tag{59}$$

$$C_{\Psi_0\psi}(\mathbf{x};\boldsymbol{\chi},\tau) = 0, \qquad \boldsymbol{\chi}\in\Gamma_D \tag{60}$$

$$n_i(\boldsymbol{\chi})\frac{\partial C_{\Psi_0\psi}(\mathbf{x};\boldsymbol{\chi},\tau)}{\partial \chi_i} + d_3(\boldsymbol{\chi},\tau)C_{\Psi_0\psi}(\mathbf{x},t;\boldsymbol{\chi},\tau) = 0, \qquad \boldsymbol{\chi}\in\Gamma_N \tag{61}$$

$$\frac{\partial^2 C_{\Psi\psi}(\mathbf{x},t;\boldsymbol{\chi},\tau)}{\partial \chi_i^2} + b_i(\boldsymbol{\chi},\tau)\frac{\partial C_{\Psi\psi}(\mathbf{x},t;\boldsymbol{\chi},\tau)}{\partial \chi_i} + c(\boldsymbol{\chi},\tau)C_{\Psi\psi}$$
$$\cdot(\mathbf{x},t;\boldsymbol{\chi},\tau) = e(\boldsymbol{\chi},\tau)\frac{\partial C_{\Psi\psi}(\mathbf{x},t;\boldsymbol{\chi},\tau)}{\partial \tau} \tag{62}$$

$$C_{\Psi\psi}(\mathbf{x},t;\boldsymbol{\chi},0) = 0, \qquad \boldsymbol{\chi}\in\Omega \tag{63}$$

$$C_{\Psi\psi}(\mathbf{x},t;\boldsymbol{\chi},\tau) = C_{\Psi}(\mathbf{x},t;\boldsymbol{\chi},\tau), \qquad \boldsymbol{\chi}\in\Gamma_D \tag{64}$$

$$n_i(\boldsymbol{\chi})\frac{\partial C_{\Psi\psi}(\mathbf{x},t;\boldsymbol{\chi},\tau)}{\partial \boldsymbol{\chi}_i} + d_3(\boldsymbol{\chi},\tau)C_{\Psi\psi}(\mathbf{x},t;\boldsymbol{\chi},\tau) = 0, \qquad \boldsymbol{\chi}\in\Gamma_N \tag{65}$$

$$\frac{\partial^2 C_{Q\psi}(\mathbf{x},t;\boldsymbol{\chi},\tau)}{\partial \chi_i^2} + b_i(\boldsymbol{\chi},\tau)\frac{\partial C_{Q\psi}(\mathbf{x},t;\boldsymbol{\chi},\tau)}{\partial \chi_i} + c(\boldsymbol{\chi},\tau)C_{Q\psi}$$
$$\cdot(\mathbf{x},t;\boldsymbol{\chi},\tau) = e(\boldsymbol{\chi},\tau)\frac{\partial C_{Q\psi}(\mathbf{x},t;\boldsymbol{\chi},\tau)}{\partial \tau} \tag{66}$$

$$C_{Q\psi}(\mathbf{x},t;\boldsymbol{\chi},0) = 0, \qquad \boldsymbol{\chi}\in\Omega \tag{67}$$

$$C_{Q\psi}(\mathbf{x},t;\boldsymbol{\chi},\tau) = 0, \qquad \boldsymbol{\chi}\in\Gamma_D \tag{68}$$

$$n_i(\boldsymbol{\chi})\frac{\partial C_{Q\psi}(\mathbf{x},t;\boldsymbol{\chi},\tau)}{\partial \chi_i} + d_3(\boldsymbol{\chi},\tau)C_{Q\psi}(\mathbf{x},t;\boldsymbol{\chi},\tau)$$
$$= -\frac{1}{K_m(\boldsymbol{\chi},\tau)}C_Q(\mathbf{x},t;\boldsymbol{\chi},\tau), \qquad \boldsymbol{\chi}\in\Gamma_N. \tag{69}$$

[16] We now show how to derive the first two moments of flux. The flux in (2) can be rewritten as

$$q_i(\mathbf{x},t) = -K_m(\mathbf{x},t)\left\{1 + Y^{(1)} + Y^{(2)} + \frac{1}{2}\left[Y^{(1)}\right]^2 + \cdots\right\}$$
$$\cdot\left\{\frac{\partial}{\partial x_i}\left[\sum_{i=0}^{\infty}\psi^{(i)}\right] + \delta_{i1}\right\}. \tag{70}$$

Collecting terms at separate order, we have

$$q_i^{(0)}(\mathbf{x},t) = -K_m(\mathbf{x},t)J_i(\mathbf{x},t) \tag{71}$$

$$q_i^{(1)}(\mathbf{x},t) = -K_m(\mathbf{x},t)\left\{J_i(\mathbf{x},t)Y^{(1)}(\mathbf{x},t) + \frac{\partial\psi^{(1)}(\mathbf{x},t)}{\partial x_i}\right\} \tag{72}$$

$$q_i^{(2)}(\mathbf{x},t) = -K_m(\mathbf{x},t)\left\{\left[\frac{\partial\psi^{(0)}(\mathbf{x},t)}{\partial x_i} + \delta_{i1}\right]\right.$$
$$\cdot\left[0.5\left[Y^{(1)}(\mathbf{x},t)\right]^2 + Y^{(2)}(\mathbf{x},t)\right]$$
$$\left.+\frac{\partial\psi^{(1)}(\mathbf{x},t)}{\partial x_i}Y^{(1)}(\mathbf{x},t) + \frac{\partial\psi^{(2)}(\mathbf{x},t)}{\partial x_i}\right\}. \tag{73}$$

It can be shown that the mean flux is $\langle\mathbf{q}\rangle = \mathbf{q}^{(0)}$ to zeroth or first order in σ, $\langle\mathbf{q}\rangle = \mathbf{q}^{(0)} + \langle\mathbf{q}^{(2)}\rangle$ to second order, and the flux fluctuation is $\mathbf{q}' = \mathbf{q}^{(1)}$ to first order. Therefore, to first order, the flux covariances are given as

$$C_{q_iq_j}(\mathbf{x},t;\boldsymbol{\chi},\tau) = K_m(\mathbf{x},t)K_m(\boldsymbol{\chi},\tau)$$
$$\cdot\left[J_i(\mathbf{x},t)J_j(\boldsymbol{\chi},\tau)C_Y(\mathbf{x},t;\boldsymbol{\chi},\tau) + J_i(\mathbf{x},t)\frac{\partial C_{Y\psi}(\mathbf{x},t;\boldsymbol{\chi},\tau)}{\partial \chi_j}\right.$$
$$\left.+J_j(\boldsymbol{\chi},\tau)\frac{\partial C_{Y\psi}(\boldsymbol{\chi},\tau;\mathbf{x},t)}{\partial x_i} + \frac{\partial^2 C_{\psi}(\mathbf{x},t;\boldsymbol{\chi},\tau)}{\partial x_i\partial\chi_j}\right], \tag{74}$$

where the covariance functions C_Y and $C_{Y\psi}$ can be derived by multiplying $Y^{(1)}(\boldsymbol{\chi},\tau)$ and $\psi^{(1)}(\boldsymbol{\chi},\tau)$ to (27), respectively, and taking the ensemble mean

$$C_Y(\mathbf{x},t;\boldsymbol{\chi},\tau) = C_f(\mathbf{x},\boldsymbol{\chi}) + H\left[-\psi^{(0)}(\mathbf{x},t)\right]H\left[-\psi^{(0)}(\boldsymbol{\chi},\tau)\right]$$
$$\cdot\langle\alpha(\mathbf{x})\rangle\langle\alpha(\boldsymbol{\chi})\rangle C_{\psi}(\mathbf{x},t;\boldsymbol{\chi},\tau)$$
$$+R\left[-\psi^{(0)}(\mathbf{x},t)\right]R\left[-\psi^{(0)}(\boldsymbol{\chi},\tau)\right]C_{\alpha}(\mathbf{x},\boldsymbol{\chi})$$
$$+H\left[-\psi^{(0)}(\boldsymbol{\chi},\tau)\right]\langle\alpha(\boldsymbol{\chi})\rangle C_{f\psi}(\mathbf{x};\boldsymbol{\chi},\tau)$$
$$+H\left[-\psi^{(0)}(\mathbf{x},t)\right]\langle\alpha(\mathbf{x})\rangle C_{f\psi}(\boldsymbol{\chi};\mathbf{x},t)$$
$$-R\left[-\psi^{(0)}(\boldsymbol{\chi},\tau)\right]C_{f\alpha}(\mathbf{x},\boldsymbol{\chi})$$
$$-R\left[-\psi^{(0)}(\mathbf{x},t)\right]C_{f\alpha}(\boldsymbol{\chi},\mathbf{x})$$
$$+H\left[-\psi^{(0)}(\mathbf{x},t)\right]H\left[-\psi^{(0)}(\boldsymbol{\chi},\tau)\right]\psi^{(0)}(\mathbf{x},t)$$
$$\cdot\langle\alpha(\boldsymbol{\chi})\rangle C_{\alpha\psi}(\mathbf{x};\boldsymbol{\chi},\tau)$$
$$+H\left[-\psi^{(0)}(\mathbf{x},t)\right]H\left[-\psi^{(0)}(\boldsymbol{\chi},\tau)\right]\psi^{(0)}(\boldsymbol{\chi},\tau)$$
$$\cdot\langle\alpha(\mathbf{x})\rangle C_{\alpha\psi}(\boldsymbol{\chi};\mathbf{x},t) \tag{75}$$

$$C_{Y\psi}(\mathbf{x},t;\chi,\tau) = C_{f\psi}(\mathbf{x};\chi,\tau) + H\left[-\psi^{(0)}(\mathbf{x},t)\right] \cdot \left[\langle\alpha(\mathbf{x})\rangle C_{\psi}(\mathbf{x},t;\chi,\tau) + \psi^{(0)}(\mathbf{x},t) C_{\alpha\psi}(\mathbf{x};\chi,\tau)\right]. \quad (76)$$

[17] It is worthwhile to note, on the basis of (42), (75), and other related equations, that the variabilities of $\psi(\mathbf{x}, t)$ and $Y(\mathbf{x}, t)$ are some complicated functions of those in the input variables f, α, Ψ_0, Ψ, g, and Q. It is also of interest to mention that although the mean equation in (32) is nonlinear, the equations governing the second moments are linear and can be solved sequentially.

4. Numerical Implementation

[18] The moment equations derived in the last section cannot, in general, be solved analytically and are therefore solved numerically in this study. The numerical implementation is facilitated by recognizing that all second moment equations have the same format except for the driving forces. We approximate the spatial derivatives by the central-difference scheme and the temporal derivatives by the implicit method [*Zhang*, 1998, 1999; *Zhang and Winter*, 1998]. The zeroth-order mean flow equation in (32) is nonlinear and thus needs to be solved in an iterative manner. Once the mean pressure head $\psi^{(0)}$ is solved, the linear equations for the second moments can be solved sequentially. Detailed discussions about the numerical implementation of similar equations are given by *Zhang* [1998, 1999] and *Zhang and Winter* [1998]. However, it is worthwhile to mention that the moment equations developed for integrated unsaturated-saturated flow involve the Dirac delta $\delta(x)$ function and its derivative. In the numerical implementation we approximate them as follows [*Arfken*, 1970]:

$$\delta(x) = \lim_{\varepsilon\to 0} a_{\varepsilon}(x), \qquad a_{\varepsilon}(x) = \frac{1}{\pi}\frac{\varepsilon}{x^2+\varepsilon^2} \quad (77)$$

$$\delta'(x) = \lim_{\varepsilon\to 0} a'_{\varepsilon}(x), \qquad a'_{\varepsilon}(x) = -\frac{2}{\pi}\frac{\varepsilon x}{(x^2+\varepsilon^2)^2}. \quad (78)$$

It can be verified that the Dirac $\delta(x)$ defined in (77) satisfies the properties of the originally defined $\delta(x)$ function.

5. Illustrative Examples

[19] In this section we attempt to demonstrate the applicability of the developed stochastic model to unsaturated-saturated flow in hypothetical soils. The log saturated hydraulic conductivity $f(\mathbf{x})$ and pore size distribution parameter α are assumed to be second-order stationary (unless stated otherwise), with an exponential covariance function

$$C_p(\mathbf{h}) = \sigma_p^2 \exp\left(-|\mathbf{h}|/\lambda_p\right), \quad (79)$$

where $p = f$ or α, σ_p^2 is the variance of p, λ_p is the correlation scale of p, and $\mathbf{h}$ is the separation vector. In section 5.4 this requirement of medium stationarity is relaxed. For simplicity, it is assumed that f and α be uncorrelated.

5.1. Infiltration in Unsaturated-Saturated Media

[20] In this example, denoted as case 1, we first try to show the validity of our mathematical derivation and numerical implementation by comparing our results with Monte Carlo simulations. We consider a rectangle grid of 20 × 60 square elements in a vertical cross section (Figure 1) having a width L_2 = 120 cm and a height L_1 = 360 cm. Thus the size of each element is 6.0 by 6.0 cm. The boundary conditions are specified as follows: no-flow at the bottom (x_1 = 0.0), a constant deterministic flux $Q = \langle Q\rangle$ at the top (x_1 = 360 cm), constant total head at the lower part of the left and right sides (H = 60 cm and H = 54 cm, respectively), and no-flow at the upper part of the left and right sides. The input parameters are given as $\langle f\rangle$ = 0.0 (i.e., the geometric mean saturated hydraulic conductivity K_G = 1.0 cm/T, where T is any time unit, as long as it is consistent with the time unit in Q), $\sigma_f^2 = 0.1$, $\langle\alpha\rangle = 0.05$ cm^{-1}, $\sigma_\alpha^2 = 2.5 \times 10^{-5}$ cm^{-2}, $\lambda_f = \lambda_\alpha = 30$ cm, $\theta_s = 0.3$, θ_r = 0.0, $\langle Q\rangle$ = −0.004 cm /T, and σ_Q^2 = 0.0. In terms of coefficients of variation, the variabilities of K_s and α are $CV_{K_s} = \sigma_{K_s}/\langle K_s\rangle = 32.4\%$ and $CV_\alpha = \sigma_\alpha/\langle\alpha\rangle = 10.0\%$, respectively. This example with relatively small variabilities in f and α is selected to ensure convergence of Monte Carlo simulations. It is well known that flow in an unsaturated-saturated system poses an interesting numerical problem. Spatial variabilities in K_s and α make it even more challenging. As a result, convergence may not be achieved for some of the realizations, especially in the case of large variabilities. A more accurate Monte Carlo study calls for more robust numerical solvers, which is, however, outside of the scope of the present work.

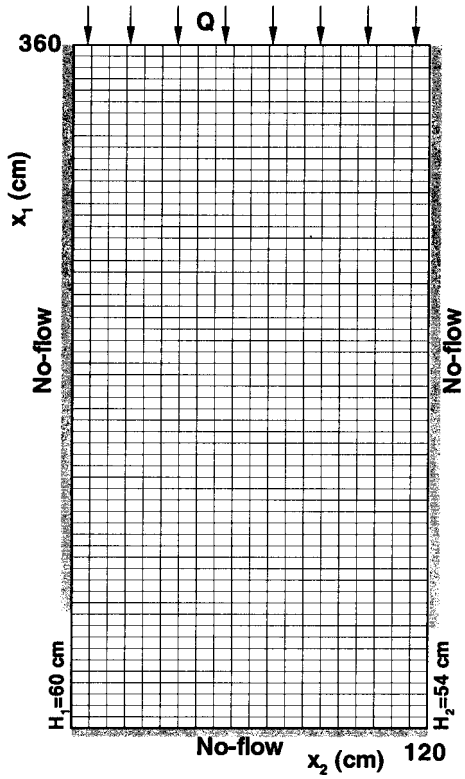

Figure 1. Boundary configuration for case 1 to case 3.

[21] Figure 2 depicts the first two moments of pressure head at steady state, obtained from the moment-equation-based stochastic model. The dotted lines in Figure 2a are equipotential lines (of total head), the solid line is the water table, and the arrowed lines are streamlines. Because the magnitude of the infiltration rate of 0.004 cm/T is much smaller than that of the mean horizontal flow component in the saturated zone (0.05 cm/T), flow has an upward component in the transition area between unsaturated and saturated zones. For the same reason, the flow in the unsaturated zone

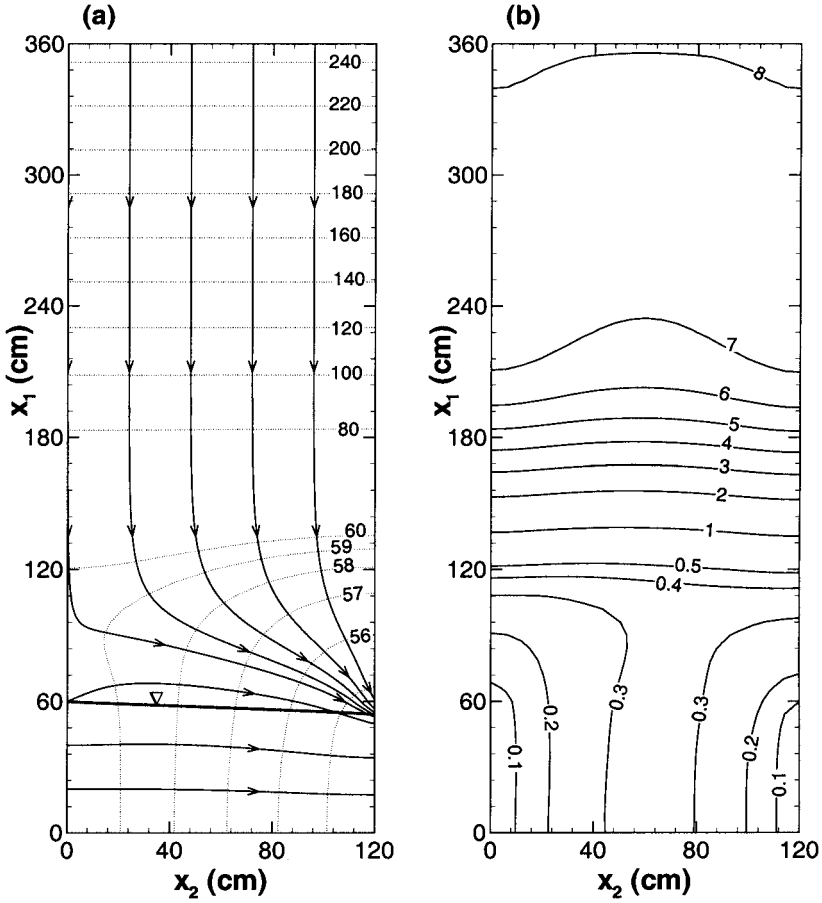

Figure 2. (a) Mean flow field for case 1, where dotted lines are equipotential lines and arrowed lines are streamlines. (b) The corresponding pressure head standard deviation.

converges to the interface of saturated and unsaturated zone at the right boundary. In the saturated zone the pressure head standard deviation is zero at the left constant head boundary and increases in the downstream direction. After reaching its maximum near the center of the saturated zone, it decreases toward zero at the right constant head boundary. Away from the water table the head standard deviation in the unsaturated zone increases quickly. Once in the mean gravity-dominated area (where the mean pressure head is constant), however, it remains unchanged until at the top flux boundary, where the deviation reaches the maximum due to the boundary effect. Compared with that in the unsaturated zone, the head standard deviation in the saturated zone is small, partially because only the variability of log hydraulic conductivity is in effect there, and partially because of the constant head boundaries in both the upstream and downstream directions. It is seen that the flow moments are strongly location dependent and the spatially nonstationary in an unsaturated-saturated system. This flow nonstationarity could not be accurately accounted for without considering the integrated flow system.

[22] For Monte Carlo simulations we generate 3000 unconditional realizations with zero mean and unit variance. The quality of random fields are then checked by comparing the ensemble covariance against the analytical covariance calculated using (79). For each simulation a log hydraulic conductivity f field and a pore size distribution α field are read from these unconditional realizations and then are scaled to the specified mean and variance of f and α. In the case that the solution does not converge, both realizations for this run are disregarded. Totally 1000 simulations are conducted, on the basis of which ensemble mean and variance are calculated. The comparison between our results (Satunsat) and Monte Carlo results (MC) is illustrated in Figure 3, showing two vertical profiles passing through the center of the flow domain. It is seen that the mean pressure head derived from our model is almost identical to Monte Carlo results (Figure 3a), while there is still some discrepancy in the pressure head standard deviation (Figure 3b). One of the plausible reasons for this discrepancy is that some of the realizations have been excluded from Monte Carlo results because the solutions do not converge, and those discarded are most likely the realizations with large contrasts in K_s and α. This may explain why the head standard deviation from the Monte Carlo simulations is smaller than that from the moment equation model. Another reason for this may be that terms of higher order are neglected in the perturbation approach. However, both profiles have a remarkably similar pattern although the standard deviation profile based on Monte Carlo simulations is slightly ragged.

[23] The increase of head standard deviation near the top flux boundary has been observed in both the moment equation model and Monte Carlo simulations. This may be explained using Monte Carlo simulations. Because the flux at the top boundary is fixed, a relatively small K_s value in a boundary element in one realization will force the boundary node to have a large total head (i.e., a small absolute value of the pressure head) to produce a relatively high head gradient. Similarly, a relatively large K_s value in the boundary element will force the boundary node to have a small total head (i.e.,

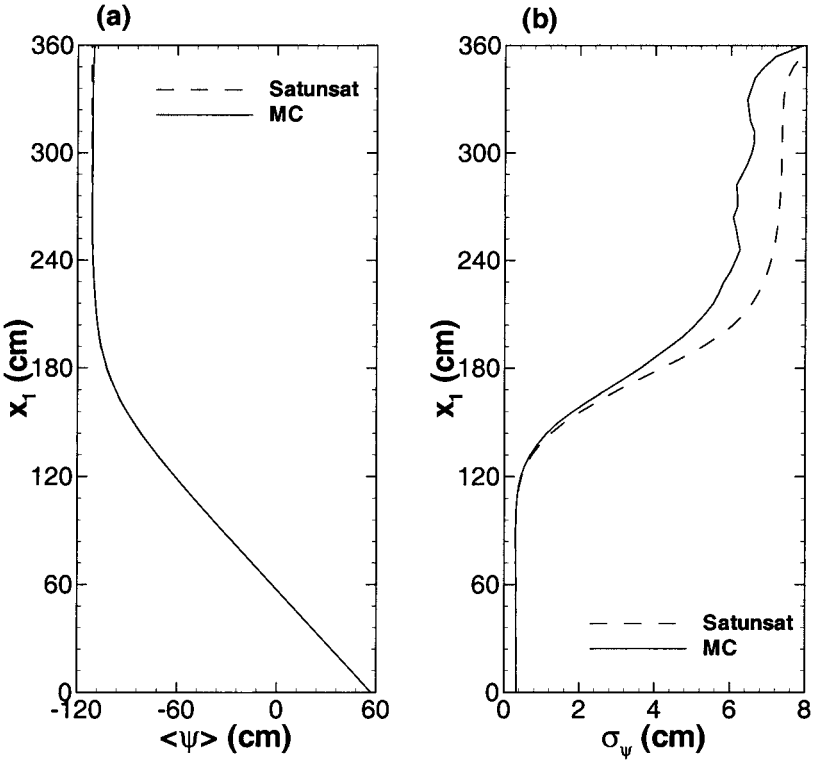

Figure 3. Comparison of Satunsat model and Monte Carlo simulation results: (a) mean pressure head and (b) pressure head standard deviation.

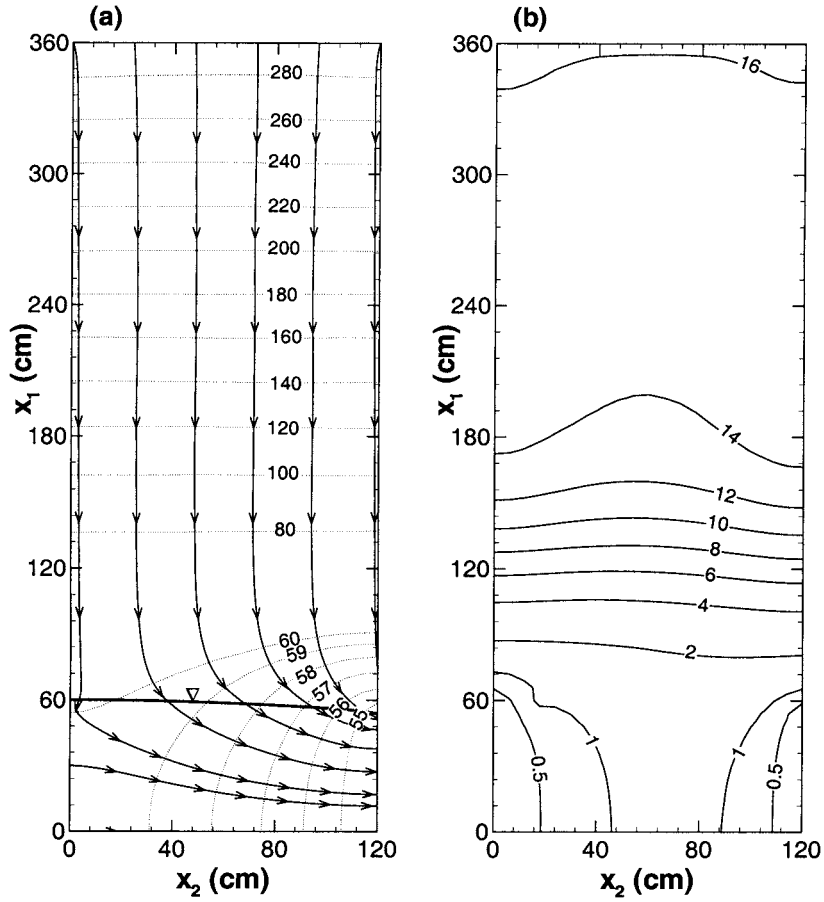

Figure 4. (a) Mean flow field for case 2, where dotted lines are equipotential lines and arrowed lines are streamlines. (b) The corresponding pressure head standard deviation.

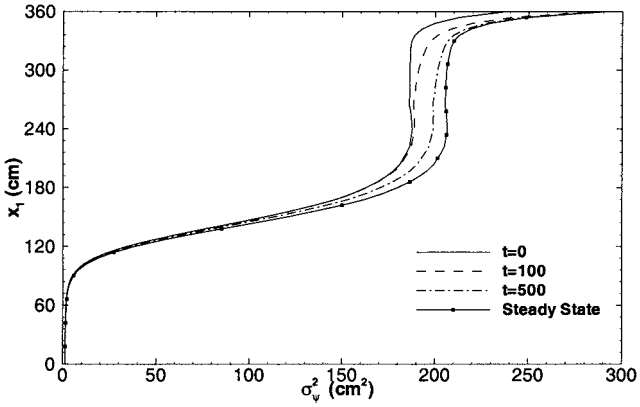

Figure 5. The propagation of pressure head variance with time, due to uncertainty in the infiltration rate.

a large absolute value of the pressure head) to produce a relatively low head gradient. Thus the variation of head at the flux boundary nodes must be larger than that in other nodes. Our moment equation model has successfully captured this phenomenon.

[24] Another way to examine the correctness of our model is to compare the first two moments of the pressure head in the mean gravity-dominated region against one-dimensional analytical results. In the mean gravity-dominated area, $\langle Q \rangle = -\exp(\langle f \rangle + \langle \alpha \rangle \langle \psi \rangle)$. For the given $\langle f \rangle = 0.0$, $\langle \alpha \rangle = 0.05$ cm^{-1} and $\langle Q \rangle = -0.004$ cm/T, the pressure head $\langle \psi \rangle = -110.43$ cm, which is close to our model results of -111.5 cm. For uncorrelated f and α, the head variance is given by *Yeh* [1989] as $\sigma^2_\psi = (\sigma^2_f + \sigma^2_\alpha \langle \psi \rangle^2)\lambda/[\langle \alpha \rangle(1 + \langle \alpha \rangle \lambda)]$, which yields $\sigma^2_\psi = 97.2$ cm^2, or $\sigma_\psi = 9.85$ cm, which is compatible with our results of 7.4 cm, considering that head variance in two-dimensional cases is smaller than the corresponding one-dimensional case. Though not shown, in the mean gravity-dominated region one-dimentional results obtained from our moment equation model are identical to the analytical solutions.

[25] We next consider a case (denoted as case 2) that has relatively large spatial variabilities: $\sigma^2_f = 1.0$, i.e., $CV_{K_s} = 131.1\%$ and $\sigma^2_\alpha = 1.0 \times 10^{-4}$ cm^{-2}, i.e., $CV_\alpha = 20\%$. The magnitude of the infiltration rate is also increased to 0.04 cm/T from the previous case of 0.004 cm/T. Given these input data, we are not able to perform meaningful Monte Carlo simulations because for many realizations of f and α, the solution for the flow problem does not converge. A carefully designed Monte Carlo simulation study is in order for such a situation.

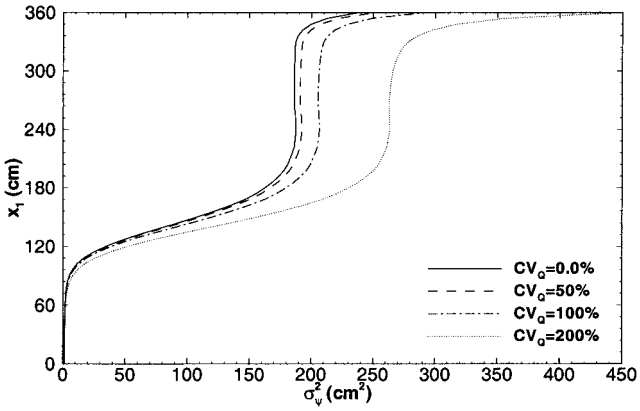

Figure 6. Distributions of the pressure head variance for different magnitudes of coefficient of variation in Q.

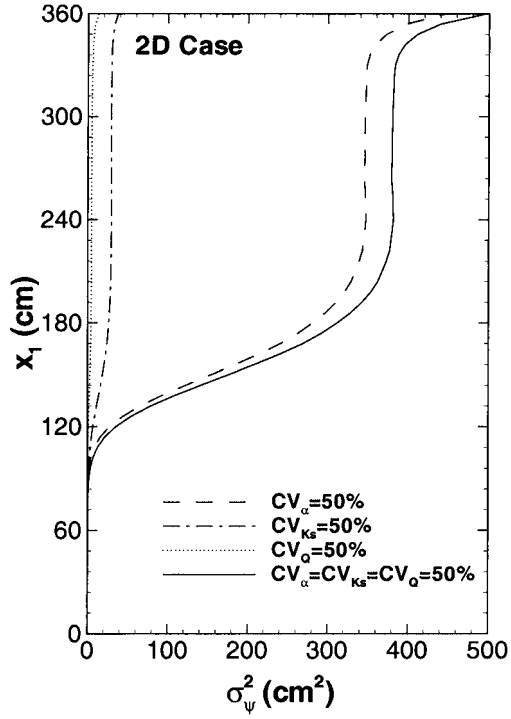

Figure 7. Relative contribution of α, f, and Q to the pressure head variance in case 4.

[26] Because the infiltration rate is compatible with the horizontal flow component in the saturated zone, the flow in the unsaturated zone directly passes through the water table and mixes with flow in the saturated zone (Figure 4a). The distribution of pressure head standard deviation is similar to that of case 1 in Figure 2b, except that in case 2, the magnitude of the pressure head standard deviation is larger than that in case 1, due to larger variabilities of f and α in case 2.

5.2. Uncertain Boundary Flux

[27] In this example (case 3) the effect of uncertainty in the infiltration rate Q on the mean flow field and the head variance is investigated. Boundary configuration and soil properties for this case are the same as those for case 2, except for the uncertainty in the infiltration rate Q. Because the variation of infiltration rate does not effect the zeroth-order mean flow field, we are only concerned with the pressure head variance. Figure 5 shows the propagation of the head variance over time, where the solid line represents the initial head variance without any uncertainty in Q and the solid line with square symbols stands for the steady state profile of the head variance with the variability $CV_Q = 100\%$. A couple of observations can be made based on Figure 5. First, the effect of variability in Q on the head variance propagates from the (top) flux boundary over time. At the early time, the pressure head variance increases only in the vicinity of the flux boundary; with time it migrates downward. After sweeping the whole unsaturated zone, it approaches the steady state, which is different from the initial state. Second, it seems that the variability in Q has little effect on the head variance in the saturated zone, even at such a large coefficient of variation of 100%.

[28] To investigate the effect of boundary flux uncertainty in more detail, we first conducted several numerical experiments with different magnitudes of the coefficient of variation in Q (Figure 6),

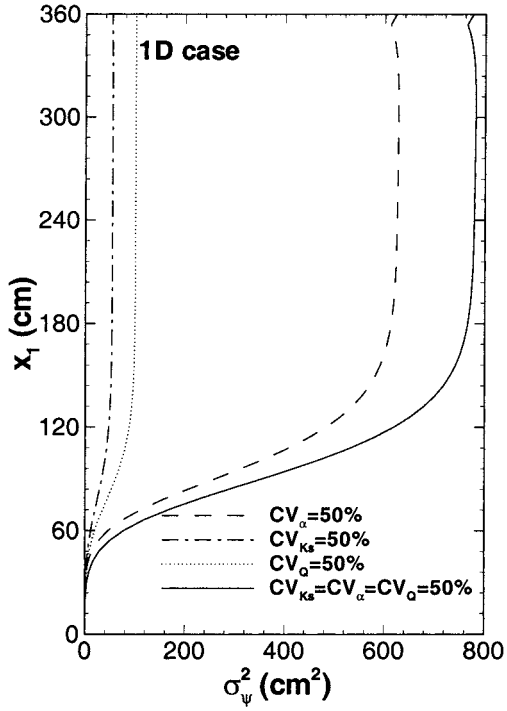

Figure 8. Relative contribution of α, f, and Q to the pressure head variance for one-dimensional unsaturated flow.

while keeping the variabilities of log hydraulic conductivity f and pore size distribution α unchanged. It is seen from Figure 6 that after excluding the effect of the variabilities of f and α, the contribution of the Q variability to the pressure head variance is linearly proportional to the square of CV_Q, i.e., linearly proportional to σ_Q^2.

[29] We also conducted three numerical simulations to investigate the relative contribution of the variability of f, α, and Q to the pressure head variance. In each simulation we only allow variation in one of these three parameters with a coefficient of variation $CV_p = 50.0\%$, where $p = K_s$, α, or Q, given $\langle f \rangle = 0.0$, $\langle \alpha \rangle = 0.05$ cm^{-1}, and $\langle Q \rangle = -0.04$ cm/T. The results are illustrated in Figure 7, where the dashed line, dash-dotted line, and dotted line represent the pressure head variance due to the variability of α, K_s, and Q, respectively. The solid line in Figure 7 stands for the pressure head variance due to the variabilities of all three parameters. It is seen that under the condition of mutually independent K_s, α, and Q, the contribution of the variability in each parameter to the pressure head variance is additive, namely, the pressure head variance due to the variabilities of all three parameters equals the sum of the three pressure head variances due to the variability of the individual parameter. In addition, it seems that the variability in the pore size distribution α has the largest contribution to the pressure head variance, compared with other parameters with the same magnitude of coefficients of variation. The finding that unsaturated flow is most sensitive to the variability in α is consistent with the earlier observations made by *Zhang et al.* [1998], where only the effects of f and α were studied. Recently, *Foussereau et al.* [2000] looked at the effect of the variability in Q on one-dimensional, transient unsaturated flow, but they did not consider the variability in α.

[30] To verify the correctness of the moment equation model, we ran three similar numerical experiments with the same parameter values but for one-dimensional unsaturated flow. The analytical solutions for pressure head variance in the mean gravity-dominated region of the unsaturated flow are available for the variabilities of f and α [*Yeh et al.*, 1985a, 1985b; *Yeh*, 1989; *Zhang et al.*, 1998]. On the basis of the numerical moment equation model (Figure 8), the contributions of the f and α variability to the pressure head variance are 53.6 and 625.0 cm^2, respectively, which are almost identical to the corresponding analytical results of 53.5 and 624.04 cm^2. The contribution of the Q variability to the pressure head variance for one-dimensional unsaturated flow in the mean gravity-dominated region can be derived by taking $x \to \infty$ in (B10) of Appendix B,

$$\sigma_\psi^2 = \frac{\sigma_Q^2}{\langle \alpha \rangle^2 \langle Q \rangle^2}. \tag{80}$$

For the parameter values given in the above, (80) yields $\sigma_\psi^2 = 100$ cm^2, which is exactly the same as the numerical result (the upper portion of the dotted line in Figure 8). Though not shown, the full profile obtained from the numerical moment equation model is identical to the analytical solution given in (B10).

5.3. Drainage in Unsaturated-Saturated Media

[31] The next example involves flow to a drain in an unsaturated-saturated system with negative pressure head at the top, impermeable boundaries at the other three sides, and a drain in the middle of the left side (similar to Figure 5.13 of *Freeze and*

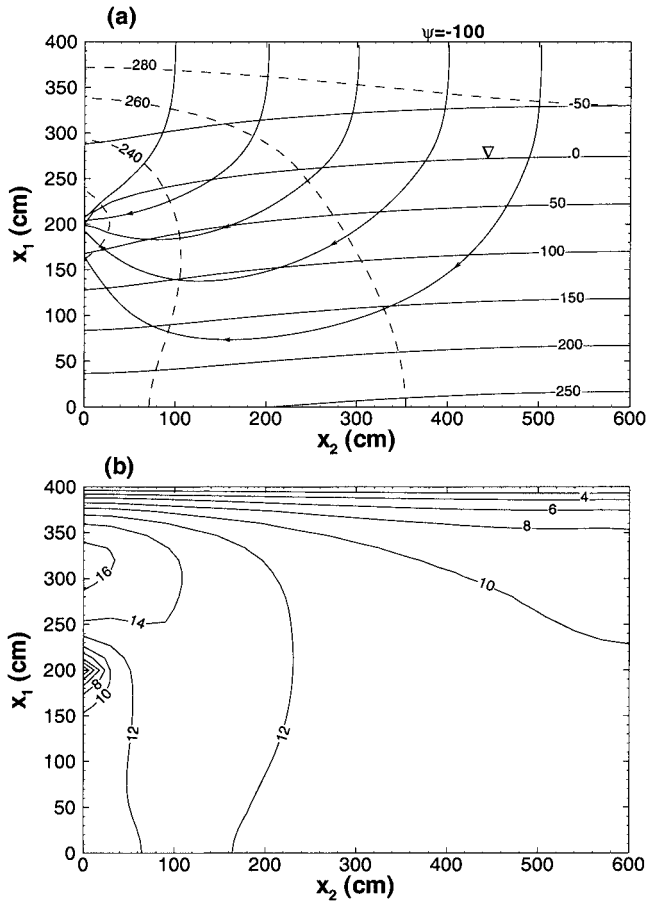

Figure 9. (a) Mean flow field for case 5, where dotted lines are equipotential lines and arrowed lines are streamlines. (b) The corresponding pressure head standard deviation.

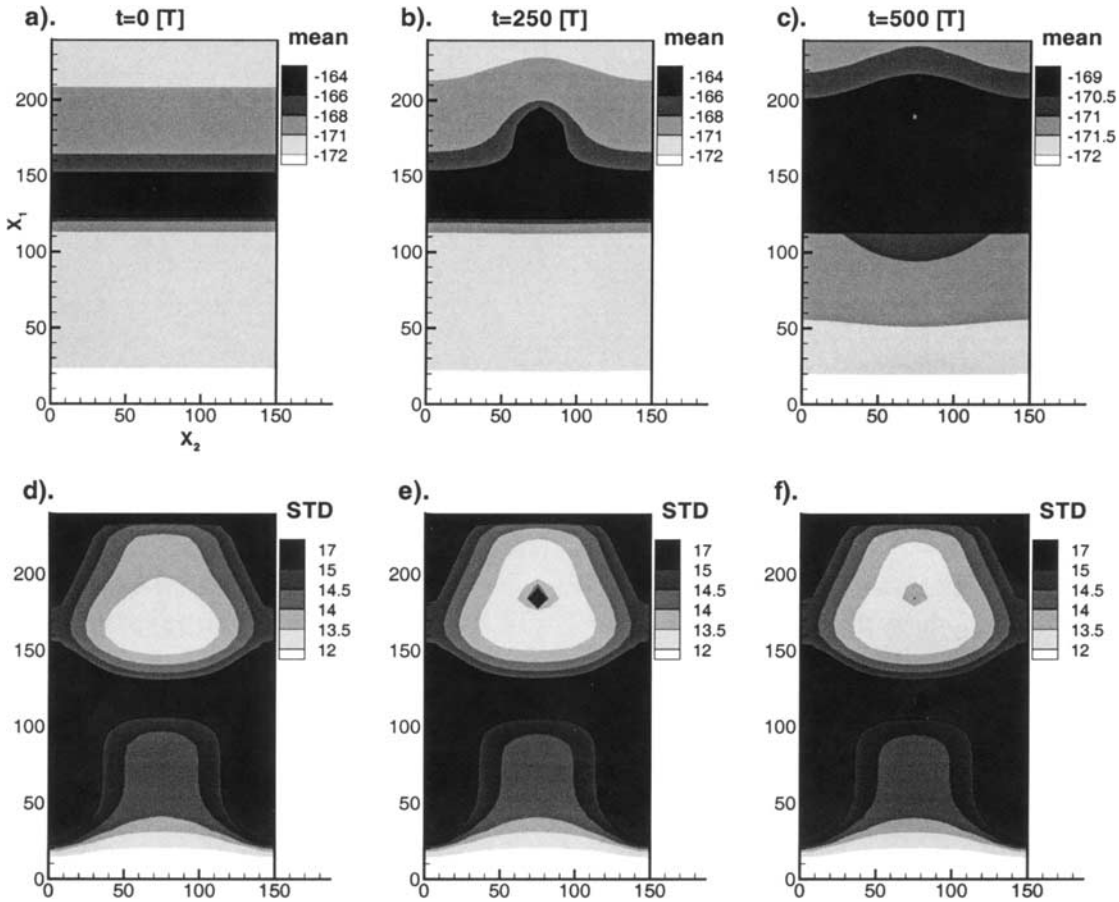

Figure 10. Contours of mean pressure head and head standard deviation at three different times in the presence of an internal source for the case of an embedded layer of coarser soils.

Cherry [1979]). The drain is implemented as a constant pressure head boundary ($\psi = 0$ cm). The flow domain with a size of 600 cm in the horizontal direction and 400 cm in the vertical direction is divided into 20 × 30 rectangle elements. The soil properties are given as $\langle f \rangle = 0.0$, $\sigma_f^2 = 1.0$, i.e., $CV_{K_s} = 131.1\%$, $\lambda_f = 50\,cm$, $\langle \alpha \rangle = 0.02$ cm^{-1}, $\sigma_\alpha^2 = 1.0 \times 10^{-4}$ cm^{-2}, i.e., $CV_\alpha = 50.0\%$, $\lambda_\alpha = 50$ cm, $\theta_s = 0.3$, and $\theta_r = 0.0$. It is assumed that f and α are uncorrelated.

[32] Figure 9a depicts the first-order mean flow field, where the solid lines are the contours of the pressure head, the dashed lines are the equipotential lines (of total head), and the arrowed lines are the streamlines. The mean flow field resembles Figure 5.13 of *Freeze and Cherry* [1979]. The standard deviation of pressure head (or total head) is shown in Figure 9b. Because the head standard deviation is zero at the upper constant head boundary ($x_1 = 400$ cm) and at the drain ($x_1 = 200$ cm) of constant head, the peak standard deviation occurs somewhere (around $x_1 = 320$ cm) between the two boundaries. In this unsaturated-saturated system, both the mean and the standard deviation of the flow quantities have complicated, nonstationary patterns, which cannot be delineated accurately without considering the coupling between the two flow regimes.

5.4. Injection in the Presence of Medium Nonstationarity

[33] The examples shown in this section involve fluid injection in an unsaturated zone embedded with a layer or zone of different soils. In this example the domain is 240 by 150 cm and represents an upper portion of an unsaturated zone. For the background soils the statistical properties are specified as $\langle f \rangle = 0$, $\sigma_f^2 = 1$, $\langle \alpha \rangle = 0.04$ cm^{-1}, $\sigma_\alpha^2 = 0.0001$ cm^{-2}, and $\lambda_f = \lambda_\alpha = 10$ cm. The boundary conditions are specified recharge (−0.001 cm/T) at the top and constant head (−172.694 cm) at the bottom, and no-flow boundaries at the two lateral sides. *Zhang* [1999], Figures 4–5 illustrated the redistribution of injected fluid in such a domain. In this study we looked at the effect of medium nonstationary features on fluid redistribution. Figure 10 shows the effects of a thin layer of slightly different soils embedded in the otherwise spatially stationary domain. This layer is of thickness 16 cm and width 150 cm with its center at $x_1 = 128$ cm. This layer has coarser soils than does the rest of the domain. In this layer the mean pore size distribution parameter is $\langle \alpha \rangle = 0.045$ cm^{-1}, compared with 0.04 cm^{-1} outside of this layer. Otherwise this case is the same as the one studied by *Zhang* [1999], Figure 4, except for the location of fluid injection. In passing, the numerical moment-equation-based approach is capable of handling other types of (more complex) nonstationary features.

[34] We first ran the system to steady state with the above mentioned boundary conditions. The steady state mean pressure head and head standard deviation contours are shown in Figures 10a and 10d. At $t = 0^+$ a source of strength $g = 0.001\ T^{-1}$ is introduced at $(x_1, x_2) = (192, 75)$ in the upper portion of the domain and lasts for 250 T. At the end of the injection, when $t = 250\ T$, the

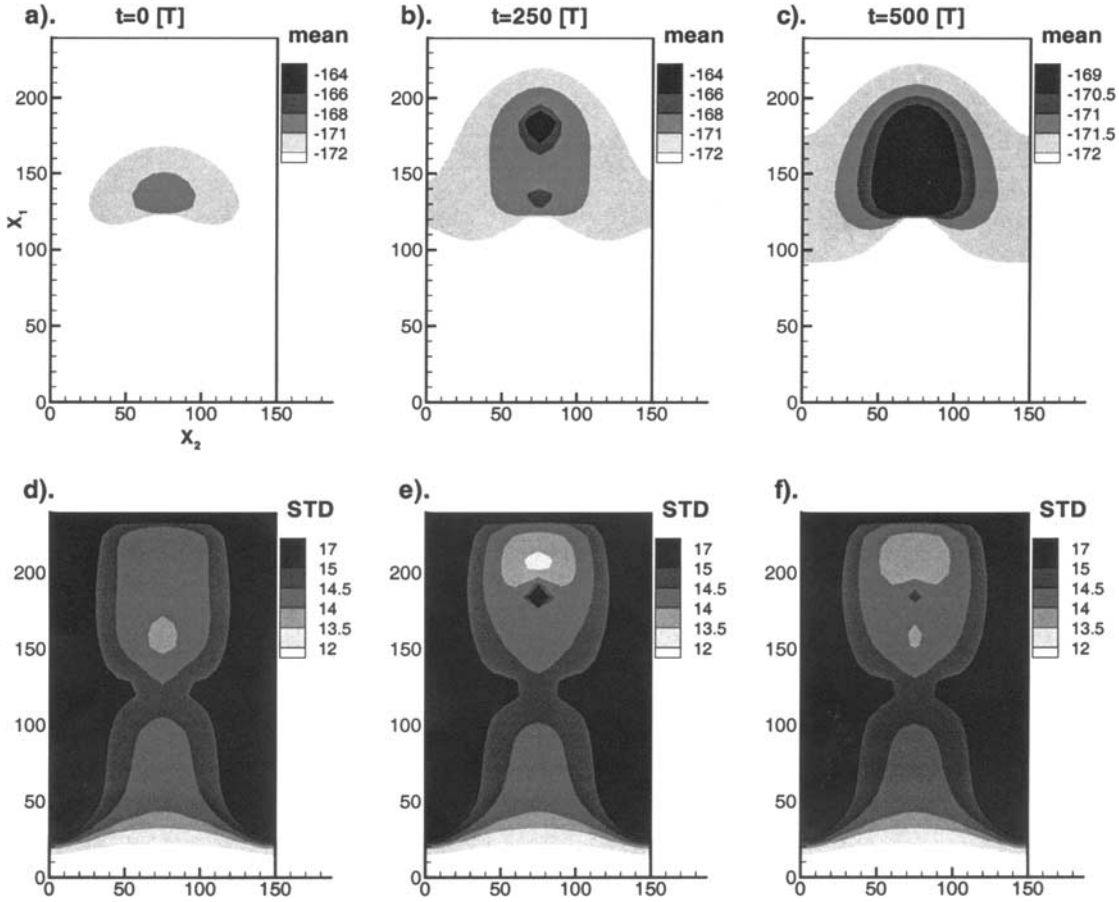

Figure 11. Contours of mean pressure head and head standard deviation at three different times in the presence of an internal source for the case of an embedded zone of coarser soils.

mean pressure head and head standard deviation contours are shown in Figures 10b and 10e, respectively. Comparison between Figure 10 and *Zhang*'s [1999] Figure 4 reveals that this nonstationary medium feature has a significant impact on the expected values of the pressure head field and the associated prediction uncertainty. First, the steady state mean flow is no longer uniform in space and is thus nonstationary (Figure 10a). The head standard deviation contours of Figure 10d are also very different from their counterparts in Figure 4d of *Zhang* [1999] for the stationary medium. At the end of injection (t = 250 T) the moisture plume moves mainly in the lateral direction above the thin layer (see Figure 10b) while it moves preferentially downward for the case of stationary medium, as shown in Zhang's Figure 4b. It is seen that this embedded layer of slightly coarser soils acts like capillary barrier, which induces lateral moisture movement but inhibits vertical migration when the layer is relatively dry. At t = 500 T the moisture starts to move vertically past the thin layer while it continues to migrate horizontally. The fluid injection renders higher pressure head standard deviation and hence a larger prediction uncertainty in the immediate vicinity of the injection point.

[35] At first glance, it is surprising that a thin layer with such a small difference in the soil properties has so significant an impact on the flow statistics. However, this result is understandable if one realizes that this thin layer is across the whole domain in the lateral direction and is thus no longer a random feature. When the size of such a feature is smaller, its effect is also less profound, as shown in Figure 11. In this figure the thin layer is only 16 cm thick and 15 cm wide with its center at (128, 75). This feature is small compared with the size of the domain but still large relative to the point source and the moisture plume, which explains why its impact on the flow moments is still relatively significant. This may suggest that whether medium features can be treated statistically without explicitly (and deterministically) considering them should depend on the scale of interest. If we are interested in flow behaviors at a pore scale, then minute features of porous media are important and flow is described by the Navier-Stokes equation. When our interest is primarily at the lab scale, the detailed flow behaviors at the pore scale are then less important and may be averaged out so that Darcy's law is appropriate. At the field scale, random features much less than this scale may be treated stochastically without explicitly accounting for them. However, if there are persistent features of significant size comparable to the domain of interest or to characteristics lengths of the flow, a nonstationary (statistically nonhomogeneous) description, such as the one utilized in this study, may be needed.

6. Summary and Discussion

[36] A first-order, nonstationary stochastic model for transient flow in both saturated and unsaturated zones is developed in this study. Because of its nonstationarity and nonlinearity, the model cannot generally be solved analytically. We solve it by the

numerical technique of finite differences, which renders the flexibility in handling different boundary conditions, medium multiscale, nonstationary features, input covariance structures, and various soil constitutive relationships. The results of the stochastic model are the first two moments (means and covariances) of the flow quantities such as pressure head and flux. The first moments estimate (or predict) the fields of pressure head and flux in a heterogeneous medium, and the corresponding (covariances) variances evaluate the uncertainty (error) associated with the estimation (prediction). These first two moments can be used to construct confidence intervals for the pressure and flux fields. In addition, the head covariance, the flux covariance, the cross-covariance between log hydraulic conductivity and head, that between unsaturated soil parameter and head, and other covariances obtained based on them may be used to derive (conditional) estimates of pressure head, log hydraulic conductivity, soil unsaturated parameters, and velocity from related field measurements by inverse methods or conditioning. Moreover, the statistical moments of the flow field are essential for studying solute macrodispersion (field-scale dispersion) because solute transport is greatly influenced by the underlying velocity field.

[37] Unlike most existing stochastic flow models that are for either saturated or unsaturated zones, the present study develops a stochastic model for integrated saturated and unsaturated systems. The two flow systems are coupled through the water table, whose position is random in randomly heterogeneous porous media. The presence of the water table renders the flow moment strongly nonstationary even in the absence of medium nonstationary features. This finding is confirmed with Monte Carlo simulations. As contaminants released at or near the land surface migrate through the vadose zone before reaching the groundwater, our integrated stochastic flow model provides the prerequisite for realistically studying contaminant transport in such a situation with a stochastic approach. Because the resulting flow moments are generally spatially nonstationary, stationary stochastic models such as those by *Dagan* [1984], *Russo* [1993], and *Destouni and Graham* [1995] are no longer applicable to transport in an integrated unsaturated and saturated system. Instead, nonstationary stochastic transport approaches are necessary [e.g., *Sun and Zhang*, 2000].

[38] Although all examples presented in this paper are unconditional, the moment-equation-based model developed in this study is also applicable to unconditional simulations, as long as the unconditional covariance function defined in (79) is replaced by conditional covariances. The latter could be obtained either from Gaussian conditioning/(cokriging) kriging or through generating and averaging a large number of conditional realizations of log hydraulic conductivity fields. With conditioning, the uncertainty of pressure head prediction can be reduced.

[39] The perturbation approach used in this study to derive moment equations is nominally restricted to small variabilities of medium properties, i.e., σ_f^2, $\sigma_\alpha^2 \ll 1.0$. However, in many cases it does work for relatively large variations in the medium properties. For example, by assuming a random constant α, *Tartakovsky et al.* [1999] have shown mathematically that the perturbation solution is asymptotic when $\sigma_f^2 \leq 2$. With a few conditioning points on hydraulic conductivity, it has been shown numerically that the perturbation approach works for $\sigma_f 2$ as large as 2 for unsaturated flow [*Lu*, 2000; *Lu et al.*, 2000] and as large as 4 for saturated flow [*Guadagnini and Neuman*, 1999b]. *Zhang and Winter* [1999] also observed an excellent agreement between the first-order moment-equation-based and the Monte Carlo approaches for the variance σ_f^2 as large as 4 in the absence of conditioning.

Appendix A

[40] Rewrite (9) as

$$Y(\mathbf{x},t) = \langle f(\mathbf{x})\rangle + f'(\mathbf{x}) - R\left[-\psi^{(0)} - \psi^{(1)} - \psi^{(2)} + \cdots\right] \cdot [\langle\alpha(\mathbf{x})\rangle + \alpha'(\mathbf{x})] = \langle f(\mathbf{x})\rangle + f'(\mathbf{x}) - \left\{R\left[-\psi^{(0)}\right] - \left[\psi^{(1)} + \psi^{(2)} + \cdots\right] \cdot \left.\frac{dR(z)}{dz}\right|_{z=-\psi^{(0)}} + \frac{1}{2}\left[\psi^{(1)} + \psi^{(2)} + \cdots\right]^2 \cdot \left.\frac{d^2R(z)}{dz^2}\right|_{z=-\psi^{(0)}} - \cdots\right\}[\langle\alpha(\mathbf{x})\rangle + \alpha'(\mathbf{x})]. \tag{A1}$$

After utilizing $dR(z)/dz = H(z)$ and $d^2R(z)/dz^2 = \delta(z)$, and collecting terms at each separate order, we have

$$Y^{(0)}(\mathbf{x},t) = \langle f(\mathbf{x})\rangle - \langle\alpha(\mathbf{x})\rangle R\left[-\psi^{(0)}(\mathbf{x},t)\right] \tag{A2}$$

$$Y^{(1)}(\mathbf{x},t) = f'(\mathbf{x}) + H\left[-\psi^{(0)}(\mathbf{x},t)\right] \left[\langle\alpha(\mathbf{x})\rangle\psi^{(1)}(\mathbf{x},t) + \psi^{(0)}(\mathbf{x},t)\alpha'(\mathbf{x})\right] \tag{A3}$$

$$Y^{(2)}(\mathbf{x},t) = \langle\alpha(\mathbf{x})\rangle H\left[-\psi^{(0)}(\mathbf{x},t)\right]\psi^{(2)}(\mathbf{x},t) + H\left[-\psi^{(0)}(\mathbf{x},t)\right]\alpha'(\mathbf{x})\psi^{(1)}(\mathbf{x},t) - \frac{1}{2}\langle\alpha(\mathbf{x})\rangle \cdot \delta\left[-\psi^{(0)}(\mathbf{x},t)\right]\left[\psi^{(1)}(\mathbf{x},t)\right]^2. \tag{A4}$$

Appendix B

[41] Here we consider one-dimensional, steady state unsaturated flow satisfying Darcy's law

$$q(x) = -K[\psi(x),\cdot]\left[\frac{d\psi(x)}{dx} + 1\right] \tag{B1}$$

subject to boundary conditions $\psi(0) = 0$ and $q(L) = Q$.

[42] Expanding (B1) by writing $\psi(x) = \Sigma_{i=0}^{\infty}\psi^{(i)}(x)$, $q(x) = \langle q(x)\rangle + q'$, and $K(x) = K_m(x)[1 + Y^{(1)} + \cdots]$, we get

$$K_m(x)\left[1 + Y^{(1)} + \cdots\right]\left(\frac{d}{dx}\sum_{i=0}^{\infty}\psi^{(i)}(x) + 1\right) = -\langle q(x)\rangle - q'(x). \tag{B2}$$

By nature of one-dimensional, steady state flow in the absence of any sink/source, we have $\langle q(x)\rangle \equiv \langle Q\rangle$ and $q'(x) \equiv Q'$. Collecting terms with the same order in (B2) gives

$$K_m(x)\left(\frac{d\psi^{(0)}(x)}{dx} + 1\right) = -\langle Q\rangle \tag{B3}$$

$$\langle q(x)\rangle Y^{(1)}(x) + K_m(x)\frac{d\psi^{(1)}(x)}{dx} = -Q'. \tag{B4}$$

[43] Substituting (26) into (B3) and solving the equation gives the zeroth-order mean pressure head

$$\psi^{(0)}(x) = \left\langle \psi^{(0)}(x) \right\rangle = \frac{1}{\langle \alpha \rangle} ln\left[-\frac{\langle Q \rangle}{K_G} + \left(1 + \frac{\langle Q \rangle}{K_G}\right) e^{-\langle \alpha \rangle x} \right], \quad \text{(B5)}$$

where K_G = exp ($\langle f \rangle$) and zeroth-order unsaturated hydraulic conductivity

$$K_m(x) = -\langle Q \rangle + (K_G + \langle Q \rangle) e^{-\langle \alpha \rangle x}. \quad \text{(B6)}$$

[44] Substituting (B6) and (27) into (B4) and assuming $f' = \alpha' = 0.0$ (i.e., only considering the variability in Q) yields

$$\frac{d\psi^{(1)}(x)}{dx} - \frac{\langle \alpha \rangle \langle Q \rangle}{K_m(x)} \psi^{(1)}(x) = -\frac{Q'}{K_m(x)}. \quad \text{(B7)}$$

Solving this equation for $\psi^{(1)}$ gives

$$\psi^{(1)}(x) = -\frac{e^{-\langle \alpha \rangle x}}{K_m(x)} \int_0^x Q' e^{\langle \alpha \rangle x'} dx'. \quad \text{(B8)}$$

The covariance of pressure head can be derived by multiplying (B8) by $\psi^{(1)}(y)$ and taking the ensemble mean,

$$C_\psi(x,y) = -\frac{\sigma_Q^2 \left(1 - e^{-\langle \alpha \rangle x}\right)\left(1 - e^{-\langle \alpha \rangle y}\right)}{\langle \alpha \rangle^2 K_m(x) K_m(y)}, \quad \text{(B9)}$$

which leads to the variance,

$$\sigma_\psi^2(x) = -\frac{\sigma_Q^2 \left(1 - e^{-\langle \alpha \rangle x}\right)^2}{\langle \alpha \rangle^2 K_m^2(x)}. \quad \text{(B10)}$$

[45] **Acknowledgments.** This work was partially funded by the LDRD project 99025 from Los Alamos National Laboratory, which is operated by the University of California for the U.S. Department of Energy. We would like to thank Jim Yeh (the associate editor for the manuscript) and the two anonymous reviewers for their constructive comments.

References

Andersson, J., and A. M. Shapiro, Stochastic analysis of one-dimensional steady state unsaturated flow: A comparison of Monte Carlo and perturbation methods, *Water Resour. Res.*, *19*(1), 121–133, 1983.

Arfken, G., *Mathematical Methods for Physicists*, 2nd ed., 815 pp., Academic, San Diego, Calif., 1970.

Bresler, E., and G. Dagan, Convective and pore scale dispersive solute transport in unsaturated heterogeneous fields, *Water Resour. Res.*, *17*(6), 1683–1693, 1981.

Brooks, R. H., and A. T. Corey, Hydraulic properties of porous media, *Hydrol. Pap. 3*, Colo. State Univ., Fort Collins, 1964.

Cushman, J. H., and T. R. Ginn, Nonlocal dispersion in media with continuous evolving scales of heterogeneity, *Transp. Porous Media*, *13*, 123–138, 1993.

Dagan, G., Solute transport in heterogenous porous formations, *J. Fluid Mech.*, *145*, 151–177, 1984.

Dagan, G., *Flow and Transport in Porous Formations*, Springer-Verlag, New York, 1989.

Dagan, G., and E. Bresler, Solute dispersion in unsaturated heterogeneous soil at field scale, I, Theory, *Soil Sci. Soc. Am. J.*, *43*, 461–467, 1979.

Destouni, G., and V. Cvetkovic, The effect of heterogeneity on large scale solute transport in the unsaturated zone, *Nord. Hydrol.*, *20*, 43–52, 1989.

Destouni, G., and W. Graham, Solute transport through an integrated heterogeneous soil-groundwater system, *Water Resour. Res.*, *31*(8), 1935–1944, 1995.

Ferrante, M., and T.-C. J. Yeh, Head and flux variability in heterogeneous unsaturated soils under transient flow conditions, *Water Resour. Res.*, *35*(4), 1471–1479, 1999.

Foussereau, X., W. D. Graham, and P. S. C. Rao, Stochastic analysis of transient flow in unsaturated heterogeneous soils, *Water Resour. Res.*, *36*(4), 891–910, 2000.

Freeze, R. A., and J. A. Cherry, *Groundwater*, 604 pp., Prentice-Hall, Old Tappan, N. J., 1979.

Gardner, W. R., Some steady state solutions of unsaturated moisture flow equations with application to evaporation from a water table, *Soil Sci.*, *85*, 228–232, 1958.

Gelhar, L. W., *Stochastic Subsurface Hydrology*, 390 pp., Prentice-Hall, Old Tappan, N. J., 1993.

Gelhar, L. W., and C. L. Axness, Three-dimensional stochastic analysis of macrodispersion in aquifers, *Water Resour. Res.*, *19*(1), 161–180, 1983.

Graham, W., and D. McLaughlin, Stochastic analysis of nonstationary subsurface solute transport, 2, Conditional moments, *Water Resour. Res.*, *25*(11), 2331–2355, 1989.

Guadagnini, A., and S. P. Neuman, Nonlocal and localized analyses of conditional mean steady state flow in bounded, randomly nonuniform domains, 1, Theory and computational approach, *Water Resour. Res.*, *35*(10), 2999–3018, 1999a.

Guadagnini, A., and S. P. Neuman, Nonlocal and localized analyses of conditional mean steady flow in bounded, randomly nonuniform domains, 2, Computational examples, *Water Resour. Res.*, *35*(10), 3019–3039, 1999b.

Harter, T., and T.-C. J. Yeh, Stochastic analysis of solute transport in heterogeneous, variably saturated soils, *Water Resour. Res.*, *32*(6), 1585–1595, 1996a.

Harter, T., and T.-C. J. Yeh, Conditional stochastic analysis of solute transport in heterogeneous, variably saturated soils, *Water Resour. Res.*, *32*(6), 1597–1609, 1996.

Hopmans, J. W., H. Schukking, and P. J. J. F. Torfs, Two-dimensional steady state unsaturated water flow in heterogeneous soils with autocorrelated soil hydraulic properties, *Water Resour. Res.*, *24*(12), 2005–2017, 1988.

Indelman, P., D. Or, and Y. Rubin, Stochastic analysis of unsaturated steady state flow through bounded heterogeneous formations, *Water Resour. Res.*, *29*(4), 1141–1148, 1993.

Kiefer, E. M., A conceptual-stochastic model of unsaturated flow in heterogeneous soils, *J. Hydrol.*, *143*, 3–18, 1993.

Li, B., and T.-C. J. Yeh, Sensitivity and moment analyses of head in variably saturated regimes, *Adv. Water Resour.*, *21*(6), 477–485, 1998.

Liedl, R., A conceptual perturbation model of water movement in stochastically heterogeneous soils, *Adv. Water Resour.*, *17*, 171–179, 1994.

Lu, Z., Nonlocal finite element solutions for steady state unsaturated flow in bounded randomly heterogeneous porous media using the Kirchhoff transformation, Ph.D. dissertion, 249 pp., Univ. of Ariz., Tucson, 2000.

Lu, Z., S. P. Neuman, A Guadagnini, and D. M. Tartakovsky, Direct solution of unsaturated flow in randomly heterogeneous soils, in *Proceedings of the XIII International Conference on Computational Methods in Water Resources*, edited by L. R. Bently, et al., pp. 785–792, A. A. Balkema, Brookfield, Vt., 2000.

Mantoglou, A., A theoretical approach for modeling unsaturated flow in spatially variable soils: Effective flow models in finite domains and nonstationarity, *Water Resour. Res.*, *28*(1), 251–267, 1992.

Neuman, S. P., C. L. Winter, and C. M. Newman, Stochastic theory of field-scale Fickian dispersion in anisotropic porous media, *Water Resour. Res.*, *23*(3), 453–466, 1987.

Osnes, H., Stochastic analysis of head spatial variability in bounded rectangular heterogeneous aquifers, *Water Resour. Res.*, *31*(12), 2981–2990, 1995.

Polmann, D. J., D. McLaughlin, S. Luis, L. W. Gelhar, and R. Ababou, Stochastic modeling of large-scale flow in heterogeneous unsaturated soils, *Water Resour. Res.*, *27*(7), 1447–1458, 1991.

Rubin, Y., Stochastic modeling of macrodispersion in heterogeneous media, *Water Resour. Res.*, *26*(1), 133–142, 1990.

Russo, D., Determining soil hydraulic properties by parameter estimation: On the selection of a model for the hydraulic properties, *Water Resour. Res.*, *24*(3), 453–459, 1988.

Russo, D., Stochastic modeling of macrodispersion for solute transport in a heterogeneous unsaturated porous formation, *Water Resour. Res.*, *29*(2), 383–397, 1993.

Russo, D., On the velocity covariance and transport modeling in heterogeneous anisotropic porous formations, 2, Unsaturated flow, *Water Resour. Res.*, *31*(1), 139–145, 1995a.

Russo, D., Stochastic analysis of the velocity covariance and the displace-

ment covariance tensors in partially saturated heterogeneous anisotropic porous formations, *Water Resour. Res.*, *31*(7), 1647–1658, 1995b.

Russo, D., and M. Bouton, Statistical analysis of spatial variability in unsaturated flow parameters, *Water Resour. Res.*, *28*(7), 1925–1991, 1992.

Shvidler, M. I., Correlation model of transport in random fields, *Water Resour. Res.*, *29*(9), 3189–3199, 1993.

Sun, A. Y., and D. Zhang, Prediction of solute spreading during vertical infiltration in unsaturated, bounded heterogeneous porous media, *Water Resour. Res.*, *36*(3), 715–723, 2000.

Tartakovsky, D. M., S. P. Neuman, and Z. Lu, Conditional stochastic averaging of steady state unsaturated flow by means of Kirchhoff transformation, *Water Resour. Res.*, *35*(3), 731–745, 1999.

van Genuchten, M. T., A closed-form equation for predicting the hydraulic conductivity of unsaturated soils, *Soil Sci. Soc. Am. J.*, *44*, 892–898, 1980.

Winter, C. L., C. M. Newman, and S. P. Neuman, A perturbation expansion for diffusion in a random velocity field, *SIAM J. Appl. Math.*, *44*(2), 411–424, 1984.

Yeh, T.-C. J., One-dimensional steady state infiltration in heterogeneous soils, *Water Resour. Res.*, *25*(10), 2149–2158, 1989.

Yeh, T.-C., L. W. Gelhar, and A. L. Gutjahr, Stochastic analysis of unsaturated flow in heterogeneous soils, 1, Statistically isotropic media, *Water Resour. Res.*, *21*(4), 447–456, 1985a.

Yeh, T.-C., L. W. Gelhar, and A. L. Gutjahr, Stochastic analysis of unsaturated flow in heterogeneous soils, 2, Statistically anisotropic media with variable α, *Water Resour. Res.*, *21*(4), 457–464, 1985b.

Zhang, D., Numerical solutions to statistical moment equations of groundwater flow in nonstationary, bounded heterogeneous media, *Water Resour. Res.*, *34*(3), 529–538, 1998.

Zhang, D., Nonstationary stochastic analysis of transient unsaturated flow in randomly heterogeneous media, *Water Resour. Res.*, *35*(4), 1127–1141, 1999.

Zhang, D., *Stochastic Methods for Flow in Porous Media: Coping With Uncertainties*, 350 pp., Academic, San Diego, Calif., 2002.

Zhang, D., and S. P. Neuman, Eulerian-Lagrangian analysis of transport conditioned on hydraulic data, 1, Analytic-numerical approach, *Water Resour. Res.*, *31*(1), 39–51, 1995.

Zhang, D., and C. L. Winter, Nonstationary stochastic analysis of steady state flow through variably saturated, heterogeneous media, *Water Resour. Res.*, *34*(5), 1091–1100, 1998.

Zhang, D., and C. L. Winter, Moment equation approach to single phase fluid flow in heterogeneous reservoirs, *Soc. Pet. Eng. J.*, *4*(2), 118–127, 1999.

Zhang, D., T. C. Wallstrom, and C. L. Winter, Stochastic analysis of steady state unsaturated flow in heterogeneous media: Comparison of the Brooks-Corey and Gardner-Russo models, *Water Resour. Res.*, *34*(6), 1437–1449, 1998.

Z. Lu and D. Zhang, Hydrology, Geochemistry, and Geology Group (EES-6), Los Alamos National Laboratory, Los Alamos, NM 87545, USA. (donzhang@lanl.gov)